Thermosensitive alternative splicing senses and mediates temperature adaptation in *Drosophila*

Naveh Evantal[1,*], Ane Martin Anduaga[2,*], Osnat Bartok[1], Ines Lucía Patop[2], Ron Weiss[1] and Sebastian Kadener[1,2,#,+]

[1] Silberman Institute of Life Sciences, The Hebrew University of Jerusalem, Jerusalem, 91904, Israel.

[2] Biology Department, Brandeis University, Waltham, MA, 02454, USA.

* These authors contributed equally to this work

[#] To whom correspondence should be addressed

Sebastian Kadener skadener@brandeis.edu

\+ Lead Contact

SUMMARY

Circadian rhythms are generated by the cyclic transcription, translation and degradation of clock genes, including *timeless* (*tim*). Currently, little is known about the mechanisms by which the circadian clock senses and adapts to temperature changes. Here we show that temperature dramatically changes the splicing pattern of *tim*. We found that at 18°C TIM protein levels are diminished due to the induction of two cold-specific splicing isoforms (*tim-cold* and *tim-short&cold*). At 29°C, another isoform, *tim-Medium* is strongly upregulated. We found that this isoform switching mechanism allows flies to regulate the levels and activity of TIM by setting miRNA-dependent thresholds for expression as well as by expressing isoforms with specific functions. Flies in which the production of *tim-short&cold* is abrogated display altered patterns of locomotor activity and altered *tim* expression. Interestingly, the introns of *tim* carry the information for the temperature sensitivity, suggesting that *tim* splicing *per se* is the temperature sensor.

KEYWORDS: circadian, *timeless,* RNA, splicing, temperature

INTRODUCTION

Circadian rhythms organize most physiological and behavioral processes to 24 hours cycles (Allada and Chung, 2010; Pilorz et al., 2018). The current model postulates that circadian clocks keep time through a complex transcriptional-translational negative feedback loop that takes place in the so-called “clock cells” (Helfrich-Forster, 2003; Shafer et al., 2006). Each one of these clock cells has been proposed to function autonomously (each cell is its own oscillator) (Dissel et al., 2014; Yoshii et al., 2012). In *Drosophila*, the master regulators CLOCK (CLK) and CYCLE (CYC) activate the circadian system by promoting rhythmic transcription of several key clock genes. Products of three of these genes, PERIOD (PER), TIMELESS (TIM), and CLOCKWORK ORANGE (CWO) repress CLK-CYC mediated transcription in an oscillatory manner (Hardin and Panda, 2013; Zhou J, 2016). These cycles of transcriptional activation and repression lead to 24-hour molecular oscillations, which ultimately generate behavioral rhythms. In addition to transcriptional control, post-transcriptional and post-translational regulatory processes play essential roles in circadian timekeeping (Hardin and Panda, 2013; Harms et al., 2004; Kojima et al., 2011; Lim and Allada, 2013). The transcriptional repressors PER and TIM are post-translationally modified, and the modification status as well as the rates with which these modifications take place have a significant influence on their degradation rates (Hardin and Panda, 2013; Ozkaya and Rosato, 2012). Modification of PER may additionally influence its transcriptional repressor activity or the timing of its activity (Hardin and Panda, 2013; Ozkaya and Rosato, 2012).

Circadian clocks are extraordinarily robust systems; they are able to keep time accurately without timing cues. In addition, and despite their biochemical nature, they are resilient to large variations in environmental conditions. The robustness of the circadian system is likely the result of multiple layers of regulation that assure accurate timekeeping and buffering of stochastic changes into the molecular clockwork. These levels of regulation are physically and/or functionally interconnected and, importantly, extend even beyond the single-cell level. Circadian neurons in the brain are organized in a network that is believed to synchronize the individual neuronal oscillators thereby contributing to a coherent and robust behavioral output

(Allada and Chung, 2010; Mezan et al., 2016; Peng et al., 2003; Schlichting et al., 2016; Stoleru et al., 2004; Weiss et al., 2014). The PDF neuropeptide, main neuromodulator of the circadian neuronal network, is expressed in a small subset of these neurons. PDF is essential for normal circadian activity patterns in light:dark (LD) cycles and for persistent circadian rhythms in constant darkness (DD) (Im et al., 2011; Peng et al., 2003; Taghert and Shafer, 2006). Circadian clocks are also remarkably plastic systems. For example, organisms can quickly adjust to different light and temperature regimes (Roessingh et al., 2015; Wolfgang et al., 2013). The plasticity of the circadian clock results from the existence of very efficient input pathways that can convey the external signals into the core oscillator machinery (Bartok et al., 2013; Ogueta et al., 2018).

Timeless is at the crossroad of both the robustness and plasticity of the circadian clock. *tim* is a core circadian oscillator component and mutations in *tim* coding sequence lead to flies with short, long, or no circadian rhythms (Myers et al., 1995; Rothenfluh et al., 2000; Sehgal et al., 1994). TIM stabilizes PER, which is also essential for circadian rhythmicity, and this complex represses CLK-mediated transcription in an oscillatory manner (Hall, 2003). Importantly, the stoichiometric relationship between PER, CLK and TIM is tightly controlled and probably the major regulator of circadian period (Fathallah-Shaykh et al., 2009; Hardin, 2011; Kadener et al., 2008; Yu et al., 2006) . In addition, TIM is the key factor for communicating external information to the central core oscillator. For example, upon light stimulus, the protein encoded by *cryptochrome*, CRY, binds to TIM and promotes TIM degradation through the ubiquitin ligase *jetlag,* which results in phase advances or delays of the circadian oscillator (Emery et al., 1998; Koh et al., 2006; Lin et al., 2001). Last but not least, PDF signalling has been proposed to synchronize the circadian clock by regulating TIM degradation (Li et al., 2014; Seluzicki et al., 2014), suggesting that TIM is the key pathway for conveying external information to the circadian system at the molecular level.

Temperature has diverse effects on the *Drosophila* circadian system (Afik et al., 2017; Kidd et al., 2015). Flies show temperature-dependent changes in the distribution of daily locomotor activity, named seasonal adaptation (Low et al., 2008; Majercak et al., 1999). They are also

entrained/synchronized by daily temperature cycles (Roessingh et al., 2015), are phase-shifted by temperature pulses or steps (Glaser and Stanewsky, 2005), and can keep 24-hour periods in a wide range of temperatures (temperature compensation (Kidd et al., 2015)). Adaptation of *Drosophila* to different environmental conditions relies on the presence of at least two neuronal circuits: one that controls the morning peak of locomotor activity (M) and another that controls the evening (E) burst of activity (Grima et al., 2004; Stoleru et al., 2004; Stoleru et al., 2005). The environment fine-tunes the activity pattern by altering the timing of these oscillators. In the laboratory, mimicking summer by subjecting the flies to hot temperatures and long photoperiods shift their M activity to pre-dawn and their E activity into the early night (Majercak et al., 1999). In contrast, under shorter day lengths and cooler temperatures, mimicking autumn, the M and E activity components fall closer together and occur around the middle of the day, enabling maximal activity at the warmest temperatures.

Work from the Edery lab in 1999 first linked the splicing of *per* 3' untranslated region (UTR) to seasonal adaptation (Majercak et al., 1999). The evening advance in locomotor activity at lower temperatures correlates with an advance in the phase of oscillation of *tim* and *per* mRNAs. The authors postulated that this shift of the clock is driven by the splicing of an alternative exon located in *per* 3' UTR. Further studies revealed that the efficiency of *per* mRNA splicing is regulated not only by temperature but also by the photoperiod (Collins et al., 2004). The effect of light on *per* splicing does not require a functional clock and phospholipase C likely plays a physiological, non-photic role in downregulating the production of the spliced transcripts (Collins et al., 2004). Moreover, in 2008, a new work examined the splicing pattern of *per* in the tropical species *Drosophila yakuba*, which faces no significant seasonal variation in day length or temperature (Ko et al., 2003; Low et al., 2008; Russo et al., 1995). Although the *per* gene of *D. yakuba* has a 3'-terminal intron, this intron is removed over a wide range of temperatures and photoperiods, consistent with the marginal effect of temperature on this tropical species. Despite these findings, it is still not clear how the regulation of the 3' UTR splicing impacts PER levels or if other transcriptional and/or post-transcriptional events are also responsible for the regulation of activity in response to temperature changes.

Post-transcriptional control by miRNAs and RNA binding proteins has been shown to be important for circadian timekeeping in flies and other organisms (Chen and Rosbash, 2016; Kadener et al., 2009; Lerner et al., 2015; Lim and Allada, 2013; Xue and Zhang, 2018). On the other hand, only more recently a few reports show a role of alternative splicing on circadian timekeeping (Bartok et al., 2013; Petrillo et al., 2011; Sanchez et al., 2010; Wang et al., 2018). This is surprising, given the prevalence of alternative splicing in the brain and the importance of this process in regulating the amount and type of mRNAs generated from a given locus (Baralle and Giudice, 2017; Sanchez et al., 2011). Alternative mRNA processing is co-transcriptional and usually happens due to the presence of suboptimal processing signals (i.e. splice or cleavage and polyadenylation sites). Many factors can influence alternative splicing including changes in RNA structure, the presence of RNA binding proteins and the elongation rate of RNA Polymerase II (Caceres and Kornblihtt, 2002; de la Mata et al., 2003).

Here we show that temperature dramatically and specifically changes the splicing pattern of *tim*. We found that the lower levels of the canonical TIM protein at 18°C are due to the induction of two cold-specific splicing isoforms (*tim-cold* and *tim-short&cold*). *Tim-cold* encodes a canonical TIM protein but it is under strong miRNA-mediated control as showed by AGO1 IP and *in vivo* luciferase reporters. Moreover, *tim-short&cold* (*tim-sc*) encodes a short TIM isoform which can advance the phase of the circadian clock when overexpressed. Interestingly, most of the changes in *tim* splicing patterns are conserved across *Drosophila* species and correlate well with the capacity of the species to adapt their activity to temperature changes. We follow by using CRISPR to generate flies in which the production of *tim-sc* is abrogated. These flies display altered patterns of locomotor activity at 18 and 25°C as well as altered expression of the remaining *tim* isoforms, demonstrating the importance of *tim-sc* production. Moreover, we showed that the temperature-dependent changes in *tim* alternative splicing are independent of the circadian clock. Furthermore, we could reproduce them in *Drosophila* S2 cells and utilizing splicing minigenes. The latter results strongly suggest that the intronic sequences of *tim* themselves are the temperature sensor for these changes in splicing.

RESULTS

Temperature remodels the circadian transcriptome

To determine the effect temperature has on general and circadian gene expression we evaluated gene expression genome-wide of heads of flies at 18°C, 25°C or 29°C. Briefly, we performed 3' sequencing at 6 different timepoints in flies entrained to 12:12 Light:Dark (LD) cycles at these three temperatures. We identified hundreds of genes displaying oscillating expression over the day (Figure 1A and Table S1). Interestingly, most of the cycling RNAs were temperature specific (Figure 1B, Table S1), with only a few RNAs consistently displaying mRNA oscillations at all the assayed temperatures. The set of oscillating mRNAs was enriched for different Gene Ontology (GO) terms, demonstrating that the circadian program is temperature dependent (Table S2). Interestingly, RNAs oscillating at 18°C display earlier phases than those cycling at 25 or 29°C (Figure 1A and Table S1). This phase advance was even more noticeable on the RNAs oscillating at more than one temperature including the core circadian components (Figure 1C), suggesting that the circadian clock gene expression program is advanced at 18°C. These phase advance mirrors the advance of the evening peak of activity observed at 18°C. Interestingly and despite the clear behavioral differences, we observed smaller phase changes in the flies entrained at 29°C compared to those at 25°C (Figure 1A, S1 and Table S1). Interestingly, our data revealed no major changes in the overall levels of most circadian components when entrained at different temperatures (Figure 1D). As stated above (and previously described (Majercak et al., 1999)), *tim* and *per* mRNA profiles were advanced at 18°C. This phase advance is transcriptional, as can be observed by assessing *tim* and *per* RNAs from nascent (chromatin-bound) RNA (Figure S2). This phase advance in the mRNA level provokes a phase advance notable in TIM and PER protein levels (Majercak et al., 1999).

To complement these data, we analyzed gene expression at the three temperatures utilizing oligonucleotide microarrays from samples that were collected at 6 timepoints but pooled before the gene expression assessment. Pooling the timepoints allows a more precise comparison of average gene expression, avoiding big variations due to timepoints. When

182 examining the Microarray data we were able to identify hundreds of mRNA transcripts that
183 change their expression in response to adaptation to different temperatures. We found
184 changes in both directions, i.e higher or lower at high/low temperatures (Figure S3A). We
185 found a number of Gene Ontology (GO) categories enriched among the differentially
186 expressed genes, spanning a wide range of biological functions (Figure S3B). These results
187 are consistent with previously reported data (Boothroyd et al., 2007a). For example, we
188 observed an increase in expression of ribosomal proteins, genes involved in protein folding
189 and metabolic processes at 29°C. At 18°C we saw increased expression of proteins involved
190 in cuticle development, which is consistent with previous reports showing that cuticle
191 deposition is temperature dependent (Boothroyd et al., 2007a; Ito et al., 2011). These results
192 demonstrate the dramatic effect that temperature has on mRNA steady-state levels and on
193 various cellular and metabolic processes. Overall, the data above demonstrates the eminent
194 role of temperature in global gene expression, and specifically on the circadian molecular and
195 transcriptional network.
196
197 ***Temperature modulates tim alternative splicing***
198 3'-seq datasets are a powerful tool for examining changes in gene expression. However, they
199 lack the ability to capture many processing events such as alternative splicing and alternative
200 promoter usage. Therefore, we generated whole-transcript polyA$^+$ RNA-seq datasets from
201 heads of flies entrained at 18°C, 25°C or 29°C. We found that temperature changes greatly
202 impact the pattern of alternative splicing of *tim* mRNA but not any other clock gene (Figure 2A
203 and data not shown). We identified four major isoforms generated from the *tim* locus (Figure
204 2B). Except for the canonical transcript, which is generated from an already characterized
205 transcript (referred to from now on as *tim-L*), all other three isoforms changed their expression
206 in a temperature dependent manner. Two of those were more abundant at 18°C compared to
207 25°C. The first one was previously described as being induced by cold temperatures (*tim-cold*)
208 (Boothroyd et al., 2007a; Wijnen et al., 2006). It includes the last intron of *tim* and has a stop
209 codon at the beginning of the intron, generating a slightly smaller protein than the canonical

tim-L isoform, but with a longer 3' UTR. The second cold-enriched isoform, although annotated, was not previously described, and we named it *tim-short&cold* (abbreviated *tim-sc*), as putatively encodes a much smaller protein. In contrast to the other isoforms which are generated by intron retention, *tim-sc* mRNA is generated by the usage of an alternative cleavage and polyadenylation site located with the intron 10 of *tim* which can only be used before this intron is spliced out. The third isoform we identified potentially encodes for a medium sized protein (smaller than those encoded by *tim-L* and *tim-cold* and larger than *tim-sc*) that we named *tim-medium* (abbreviated *tim-M*). This isoform was recently described and named *tim-tiny* (Shakhmantsir et al., 2018). However, to avoid confusion with *tim-sc* (which encodes an even smaller isoform), we will call this isoform *tim-M.* This isoform, is generated by the inclusion of an intron containing a stop codon and shares all downstream exons with *tim-L*, hence presenting the longest 3' UTR of all isoforms. We found that this isoform is highly expressed in flies entrained to 25°C or 29°C compared to flies kept at 18°C.

Since three of these isoforms (*tim-L, tim-cold and tim-M*) share the same 3' end, they are undistinguishable in the 3'-seq datasets. In contrast, we could easily detect a significant increase in the levels of *tim-sc* mRNA at 18°C in this dataset (Figure S4). We also could observe the effect in the whole-transcript datasets, although the differences were more difficult to appreciate due to the underrepresentation of 3' ends in whole-transcript sequencing. We confirmed the changes detailed above by qRT-PCR using isoform specific primers (Figure S5A). Importantly, the levels of *tim-L* cannot be unequivocally assessed by qPCR as its sequence overlaps with *tim-M.* Temperature-dependent changes in the splicing patterns of *tim* are, at least, as impressive as the previously described changes in the splicing of a small intron in the 3' UTR of *per* (Majercak et al., 1999).

We next utilized the whole RNA-seq datasets to quantify the relative amount of each of the four isoforms (Figure 2C). We found the change in the distribution of the four isoforms between the different temperatures to be clearly dramatic, from a fairly even distribution at 18°C to no expression of *tim-sc* and *tim-cold* and significant elevation of *tim-M* at 29°C. Surprisingly, we found that *tim-M* constitutes about fifty percent of *tim* mRNAs at 25°C, having a similar, if not

238 higher, expression than the canonical isoform *tim-L.* This suggests the existence of previously
239 unknown aspects of *tim* regulation even in canonical conditions. In comparison to the big
240 changes driven by temperature observed in *tim* alternative splicing, the well-characterized
241 changes in *per* alternative splicing are very modest (Low et al., 2008) (Figure2D). To assess
242 if the observed changes in *tim* RNA processing upon temperature changes also happen in the
243 fly brain, we dissected the brains of flies entrained at 18, 25 and 29°C and measured the levels
244 of each *tim* isoform by qPCR. As observed when utilizing fly heads, entrainment of the flies to
245 lower temperatures (18°C) resulted in a strong increase of *tim-s* and *tim-cold* levels while
246 higher temperatures (29°C) promoted *tim-M* expression (Figure S5B).
247
248 ***Temperature-specific alternative splicing is conserved across Drosophilae* and**
249 ***correlates with temperature adaptation***
250 If changes in the splicing pattern of *tim* are necessary for temperature adaptation, it should be
251 conserved among other *Drosophila* species that adapt to temperature changes. Therefore, we
252 determined both the behavioral and splicing patterns of three additional species, belonging to
253 the *Drosophila* genus at 18, 25 and 29°C. Two of those species (*D.simulans* and *D.Yakuba*)
254 belong, like *D.melanogaster,* to the *Sophophora* subgenus, while the third (*D.virilis*) belongs
255 to the *Drosophila* subgenus. Furthermore, even if they share the same tropic origin,
256 *D.melanogaster* and *D.simulans* have become cosmopolitan, while the distribution of
257 *D.Yakuba* is restricted to Africa (Kuntz and Eisen, 2014; Markow and O'Grady, 2007). *D.virilis*,
258 a Holarctic species, is also geographically temperate. Although all species displayed some
259 degree of behavioral adaptation to temperature, we could detect differences between species
260 when analyzing the ratio between light and dark activity in all three temperatures (Figure 3A).
261 As expected, *D.melanogaster* displays a temperature-dependent gradient in the day/night
262 activity ratio, with highest ratios at 18°C (Figure 3A, left). *D.simulans* showed the same trend
263 of significant decrease in light/dark activity ratios in elevating temperatures, suggesting
264 behavioral adaptation to high and low temperatures (Figure 3A, middle-left ; Figure S6A upper
265 left panel and data not shown). In contrast, while adjusting to high temperatures, *D.Yakuba*

did not show any significant difference between the ratios of 25°C and 18°C, suggesting reduced adaptational capacity to lower temperatures (Figure 3A, middle-right; Figure S6A middle left panel and data not shown). It should be mentioned that while the ratio at 29°C in *D.virilis* is the same as in the other species, its activity was affected in the opposite trend than the others, decreasing during the dark (Figure 3A, right ; Figure S6A lower left panel and data not shown).

We followed by generating whole-transcript polyA$^+$ RNA-seq datasets from the heads of all three species entrained at the 3 different temperatures. When examining the splicing pattern of *tim*, we could see that all species displayed dynamic changes in *tim-cold* and *tim-M* in response to temperature changes, with *tim-cold* increasing and *tim-M* decreasing at lower temperatures (Figure 3B and Figure S6). This suggests that these changes might be important for the behavioral changes shared by all species. However, we only detected *tim-sc* in *D.simulans* and *D. melanogaster*, which had very similar temperature-dependent alternative splicing profiles (Figure 3B and Figure S6). As mentioned above, this isoform appears only at 18°C, strongly suggesting that this isoform is responsible for the adaptation to cold temperatures, which is shared between *D.simulans* and *D.melanogaster.* The results displayed above showed a strong correlation among the different fly species between the changing on *tim* mRNA isoforms and the capacity to adapt to colder temperatures. We also looked at changes in *per* 3' UTR splicing in the different species between temperatures. *D.virilis* displayed no changes in *per* splicing, while the changes in *D.Yakuba* were mild, in both cases the spliced isoform dominated (Figure 3B and Figure S6B).

Cold temperature decreases TIM-L levels by two independent mechanisms

As previously described (Majercak et al., 1999), we found that the levels of TIM-L protein are significant downregulated at 18°C compared to 25°C or 29°C. We could not clearly detect or differentiate the other isoforms by Western Blot (data not shown). Nevertheless, TIM-COLD has been reported to be expressed by Boothroyd et al. (2007a). *tim-M* mRNA is very abundant but we could not see a protein of the predicted size in the western blotts, which strongly

suggests that that this isoform is poorly and/or not translated. Hence, expression of this isoform could serve as a way to regulate the amount of *tim-L* production. This agrees with a recent publication that identified this mRNA isoform as non-coding (Shakhmantsir et al., 2018). We also could not univocally detect TIM-SC. While we observed bands of TIM-SC expected size in the TIM immunoblot, these bands are present at all temperatures (data not shown). We believe that these bands might represent canonical TIM degradation products of similar size than TIM-SC (see below). In addition, the utilized TIM antibody was raised against the whole protein and detects TIM-SC with low efficiency (see below).

Interestingly, the lower levels of TIM-L at 18°C are not due to changes in total *tim* mRNA, as observed in our datasets (Figure S4) and reported by others (Boothroyd et al., 2007b). This suggests that the lower TIM levels are due to post-transcriptional and/or post-translational regulation. miRNA-mediated repression is one of the most common mechanisms of post-transcriptional control. Moreover, recent work demonstrated that *tim* mRNA is regulated by miR-276 (Chen and Rosbash, 2016). We then decided to determine whether *tim* is regulated by miRNAs in a temperature dependent way. To do so, we tested the genome-wide association of mRNAs with the ARGONAUTE 1 (AGO1, the only miRNA-RISC effector protein in *Drosophila* (Förstemann, Horwich, Wee, Tomari, & Zamore, 2007) at 18°C, 25°C and 29°C. Briefly, we performed AGO1 immunoprecipitation (IP) from fly heads followed by hybridization to oligonucleotide microarrays. In these datasets, we can only assess overall *tim* levels (as these microarrays cannot distinguish between *tim-L, tim-cold* and *tim-M*). We first confirmed that the overall distribution of AGO1-associated mRNAs (and hence miRNA-mediated regulation) is similar at all three temperatures (Figure S7). Interestingly, we observe changes in the association of *tim* to AGO1 (Figure 4A). Binding of *tim* to AGO1 is very strong at 18°C while there is very little or no association at 25 or 29°C. This patter is *tim*-specific and, when examining other core circadian clock components, we could not see such temperature-driven AGO1 association changes. Some are bound at all temperatures (like *Clk* or *vri)* and some do not bind at all (like *cry, cyc* and *per;* Figure 4A). Importantly, the probes in the oligonucleotide microarray do not allow distinguishing between *tim-L, tim-cold* and *tim-M*. To determine

whether the association of the different *tim* transcripts to the miRNA-effector machinery is temperature dependent, we performed isoform-specific qPCRs from newly generated AGO1-IP samples. While the mRNA encoding the transcription factor CBT (a known miRNA-regulated RNA (Kadener et al., 2009; Lerner et al., 2015)) was strongly bound to AGO1 in all the assayed temperatures, we discovered that the association of *tim-L/M, tim-cold* and *tim-M* to AGO1 was significantly higher at 18°C (Figure 4B).

To determine the consequences of AGO1 binding on TIM expression, we generated flies carrying luciferase reporters fused to the different 3' UTRs of *tim*. All transgenes were targeted and inserted in the same genomic location, and we expressed these UAS-transgenes using the *tim-gal4* driver. To minimize the effects of temperature on the GAL4 transgene, we performed the experiment at 25°C. The Luciferase levels of the transgenes carrying the 3' UTRs of *tim-L* and *tim-sc* were high, suggesting little (or no) post-transcriptional control, at least at 25°C. Interestingly, the reporter carrying the 3' UTR of *tim-cold* showed a strong decrease of Luciferase levels compared to the rest of the reporters, suggesting that the presence of this 3' UTR strongly diminishes the translation potential of this isoform either by affecting the stability of the mRNA or, directly, by preventing its translation (Figure 4C). Similarly, the *tim-M* 3' UTR reporter displayed lower luciferase levels, although the effect was milder than the one observed with *tim-cold* 3' UTR.

To further understand the post-transcriptional regulation of *tim,* we analyzed the different 3' UTRs for potential miRNA binding sites using Target Scan (Agarwal, Bell, Nam, & Bartel, 2015). Three of the isoforms, *tim-L, tim-cold* and *tim-M* contain a large number of miRNA binding sites, many of which are evolutionary conserved and highly expressed in fly heads (Table S3). *Tim-sc* contains only 5 miRNA binding sites and was not bound to AGO1 at any temperature demonstrating it is not regulated by miRNAs (Figure 4D).

The miRNAs responsible for the association of *tim* isoforms with AGO1 could target only a temperature-specific isoform, more than one isoform, be expressed in a temperature-dependent way or a combination of these. We therefore sequenced AGO1-associated miRNAs from heads of flies entrained to 12:12 LD cycles at 18, 25 and 29°C. While the

expression of most miRNAs was not affected by temperature, a few of them were (Figure 4E, Table S4). We first focus on the miRNAs targeting the 3' UTR region common to *tim-L, tim-cold* and *tim-M.* Of the 17 miRNAs predicted to target this region, only two change with temperature. One of them (miR-33) is modestly increased at 29°C in comparison with 18C. Notably miR-969, which contains a strong binding site in this 3' UTR, is strongly (~3 fold) upregulated at 18°C, with intermediate expression at 25°C and low at 29°C (Figure 4F). Changes in the abundance of this miRNA might explain the temperature dependent association of *tim-L* to AGO1. However, *tim-M* and *tim-cold* contain additional 3' UTR regions and these regions are predicted to be targeted by other miRNAs that are strongly regulated by temperature. For each of these *tim* isoform, half of the miRNAs predicted to bind them are highly expressed at 18°C and half highly expressed at 29°C (Figure 4F and Tables S3 and S4). This strongly suggests the existence of a mechanism for downregulating TIM-COLD and TIM-M at all temperatures. The fact that TIM-COLD is indeed present at 18°C (Boothroyd et al., 2007a; Wijnen et al., 2006), suggest that the main function of the miRNA-mediated regulation of this isoform is to impose a threshold for avoiding expression of this protein at temperatures other than 18°C.

In sum, these results, strongly suggest that, at 18°C, changes in the canonical TIM protein are due to the deviation of *timeless* transcription towards the production of a short isoform (*tim-sc*) and another isoform under strong post-transcriptional regulation (*tim-cold*). In addition, at this temperature even *tim-L* is subjected to a stronger post-transcriptional control by miRNAs. Last, *tim-M* is also regulated post-transcriptionally at all temperatures (similar to *tim-cold*).

Overexpression of the different TIM isoforms alters circadian behavior differently

We next sought to determine the functionality of the different TIM isoforms. To do so we generated plasmids expressing the different TIM protein isoforms fused to a C-terminal FLAG tag and the same 3' UTR under the control of the UAS-transgene (Figure S8A). To verify the expression of TIM from these plasmids we co-transfected each one of them into *Drosophila* S2 cells (which do not express *tim*) together with a GAL4 expressing plasmid. As expected,

using an anti-FLAG antibody we observed the bands of predicted size for TIM-SC, TIM-M, TIM-COLD and TIM-L (Figure S8B left). Interestingly, anti-TIM antibodies can efficiently detect TIM-L and TIM-COLD but barely detected TIM-SC (Figure S8B right). Moreover, we observed a degradation product that overlaps with TIM-SC, demonstrating that it is very difficult (if not impossible) to detect this isoform univocally by western blot. We followed by generating flies containing these plasmids by targeting them into the same *attB* insertion site, in order to obtain flies that can express the proteins at similar levels. We then over-expressed each of these TIM protein isoforms using the *tim-gal4* driver and determined the locomotor activity patterns of these flies at 25°C. When kept under a 12:12 LD cycle, we observed a clear advance in the start of the evening activity peak in the *tim-sc* overexpression flies compared to the *tim*-Gal4 control (Figure 5A, B). This, together with the fact that in DD overexpression of TIM-SC led to a one hour shortening of the period compared to the control (Figure 5C), suggests a role for *tim-sc* mRNA and protein in the behavioral advance observed in *wild type* flies at 18°C. Additionally and as previously described by Yang and Sehgal (2001), overexpression of TIM-L at 25°C resulted in a high percentage of flies displaying long, weak or no rhythms in DD conditions (Figure 5C). Overexpression of TIM-COLD also resulted in weak and/or longer rhythms although at a lower degree than TIM-L, which suggests that the two proteins are not fully equivalent (although both are functional). Surprisingly, overexpression of TIM-M did not significantly change the locomotor activity pattern neither in LD nor in DD, suggesting that this protein is non-functional (Figure 5).

Elimination of tim-sc results in changes in tim processing and locomotor activity

To definitively establish whether *tim-sc* is functional, we generated flies in which the cleavage and polyadenylation site used for the generation of *tim-sc* mRNA is mutated by CRISPR (40A flies, Figure 6A). As expected, these flies do not express *tim-sc* at any temperature (see qPCR in Figure 6B). We followed by assessing the locomotor behavior of 40A mutants and their isogenic controls. Control flies presented two different responses when transferred to 18°C: an advance of the evening peak as well as a decreased night activity in comparison to the

406 flies maintained at 25°C (Figure 6C, 6D and 6E). In addition, the activity patterns of the 40A
407 flies are strikingly similar at the different temperatures. At 18 and 25°C, 40A mutants display
408 lower activity than control flies only during the night while at 29°C, these 40A flies were less
409 active both in the light and dark periods (Figures 6D and S9). Even more importantly, and
410 opposite to TIM-SC overexpression, 40A mutants display a significant delay in the time of
411 evening activity onset specially at 18°C but also more mildly at 25°C (Figures 6C and 6E).
412 Finally, we measured the levels of the other *tim* isoforms in control and 40A flies at 18, 25 and
413 29°C in order to assess the molecular consequences of the disruption of *tim-s* production.
414 *Tim-sc* mutant flies do not show changes in the overall levels of *tim* mRNA (as assessed by
415 determining the levels of the constitutive exon 5 and 6; Figure 6F left). However, elimination
416 of *tim-sc* results in an increase in the levels of *tim-cold* both 18 and 25°C at the maximum
417 expression timepoint (ZT15; Figure 6E). *tim-L/M* levels also are increased in the mutant, but
418 only at 25°C.
419 These results strongly suggest that both TIM-SC protein and *tim-sc* production can regulate
420 the daily pattern of locomotor activity and the response to temperature changes. Importantly,
421 we still observe some degree of temperature adaptation in 40A mutants, which we postulate
422 are mediated by the increased production of *tim-cold*.
423
424 ***Tim alternative splicing is regulated directly by temperature in-vitro and in-vivo***
425 To get insights into the mechanism by which temperature regulates *tim* alternative splicing,
426 we determined if tim^{01} and per^{01} mutants also change *tim* alternative splicing in a temperature-
427 dependent way. Hence, we entrained control and both mutant lines in LD conditions at 18°C
428 and at 29°C, collected flies every four hours, extracted RNA from fly heads from a mix of all
429 time points and performed qPCR. We observed a similar trend in all three fly lines, namely:
430 an increase in *tim-cold* and *tim-sc* and a decrease in *tim-M* at 18°C (Figure 7A). This
431 demonstrates that, as previously shown for *per* temperature-dependent splicing, *tim*
432 thermosensitive splicing events are independent of the circadian clock.

The splicing sites flanking alternatively spliced exons are usually weaker and temperature is known, at least *in vitro*, to strongly influence the efficiency of splicing. Hence, we determined the strengths of the different splice sites in *tim* using a publicly available software (Reese et al., 1997). Almost all *tim* constitutive introns exhibited strong 5' and 3' splice site strengths (above 0.6 scores, Figure S10). Interestingly, the introns retained in *tim-M* and in *tim-cold* have strong 5' splice sited and a weak 3' splice site. This suggests that at least part of the mechanism underlying the production of these isoforms is due to the presence of weak 3' splice sites. However, the splice sites of the intron associated with *tim-sc* bear strong 5' and 3' splice site (**Figure S10**), suggesting that the increase of *tim-short* at lower temperatures might be the result of a more efficient cleavage and polyadenylation rather than changes on the splicing efficiency. In addition, we observed that *D.melanogaster*, *D.simulans* and *D.Yakuba* possess strong 5' splice sites and weak 3' splice sites of the introns retained in *tim-cold* and *tim-M* whose alternative splicing is temperature sensitive in these species (Figure S10). Interestingly both *tim-cold* and *tim-M* respond in opposite ways to changes in temperatures (with *tim-cold* strongly retained at 18°C and *tim-M* more skipped at this temperature).

Tim was one of the few genes in which we observed temperature dependent changes in alternative splicing (data not shown). Hence, it is possible that *tim* alternative splicing *per* se could be thermosensitive. To test this possibility, we utilized the embryonic cell line Schneider 2 (S2 cells). These cells do not express most circadian components including *Clk, per* and *tim*. However, *tim* expression can be induced by expression of CLK (McDonald & Rosbash, 2001). So, we transfected these cells with a plasmid driving expression of *Clk*. We used an inducible vector in order to bypass any transfection variation that might arise due to different temperature conditions (Lerner et al., 2015). After the induction of *Clk,* we cultured the cells either at 25°C or 18°C for 24 hours. We then collected the cells, extracted RNA and characterized the splicing pattern of *tim* by qPCR. For each of the alternative isoforms, we measured the ratio between the unspliced and spliced variants and compared these ratios between the two temperatures. Indeed, we completely reproduce the results obtained *in* vivo,

namely: *tim-cold* and *tim-sc* were higher at 18°C, while *tim-M* showed the opposite trend (Figure 7B). However, we did not observe any temperature-induced changes of a constitutive *tim* exon (Control, Figure 7B) demonstrating that this effect is specific for the thermosensitive introns.

One intriguing possibility is *tim* splicing *per se* functioning as a thermometer. This could be accomplished if temperature could, for example, expose binding sites for a specific splicing factor or if the splicing of these introns is temperature dependent. To test this possibility, we generated three different *tim* minigene reporters consisting of the exons and intron involved in each event of *tim* alternative splicing (Figure 7C). As observed *in vivo* and in the context of the whole *tim* gene in S2 cells, we observed a temperature-dependent effect on the splicing of the three different *tim* minigenes. We did not observe any temperature dependence in the splicing of a minigene generated from a constitutive exon (Figure 7D), demonstrating a direct effect of temperature on *tim* alternative splicing.

DISCUSSION

In this study we show that temperature dramatically and specifically changes the splicing pattern of the core circadian component *timeless*. We found that the lower levels of the canonical TIM (TIM-L) protein at 18°C are due to the induction of two cold-specific splicing isoforms (*tim-cold* and *tim-short&cold*). *Tim-cold* encodes a protein very similar to TIM-L but it is under strong post-transcriptional control, as showed by AGO1-IP and *in vivo* luciferase reporters. Moreover, *tim-sc* encodes a short TIM isoform which results in an advanced phase of the circadian clock when overexpressed. Interestingly, these changes in *tim* splicing patterns are conserved across several *Drosophila* species and correlate well with the capacity of the species to adapt their activity to temperature changes. We then generated flies in which the production of *tim-sc* is abrogated. These flies display altered patterns of locomotor activity at 18°C and 25°C as well as altered expression of the remaining *tim* isoforms demonstrating the importance of *tim-sc* production. Last, we showed that the temperature-dependent changes in *tim* alternative splicing are independent of the circadian clock. Moreover, we could reproduce them in *Drosophila* S2 cells either promoting endogenous *tim* expression using the p-Act-*Clk* plasmid or utilizing splicing minigenes. The latter results strongly suggest that *tim* intronic sequences themselves are the temperature sensor for these splicing changes.

The fact that despite being the most abundant RNA isoform, we could not detect TIM-M suggests that this RNA is poorly (or not) translated. Alternatively, the protein could be quickly degraded. However, the protein is fairly stable as we could detect large amounts of TIM-M upon overexpression (Figure S8). Moreover, our luciferase reporter experiments suggest that little protein is produced from this RNA, likely by regulation by miRNAs. It is also possible that this RNA isoform is not even exported from the nucleus and nuclear/cytoplasmic fractionation experiments could be useful to test this possibility. Regarding *tim-cold,* this isoform is strongly regulated by mIRNAs at all temperatures and was reported (Montelli et al., 2015) to display weaker binding to CRY in yeast. Our results with the *tim-sc* null mutant provide support for a specific (and even dominant) function of TIM-COLD. We observed that *tim-sc* mutants have increased levels of *tim-cold* mRNA at 25°C. At this temperature these flies behave as if they

were at lower temperature (low daytime activity and advanced evening peak of activity). Similar to *tim-cold, tim-sc* seems to work both at the RNA and protein levels. On one hand, the increase in the production of *tim-sc* at 18°C helps regulate the amount of *tim-L* and *tim-cold* produced at this temperature (Figure S8). In addition, overexpression of TIM-SC advances the phase and shortens the period of the circadian clock, suggesting that expression of this isoform might mediate some of the changes seen upon introduction of flies at 18°C. An accompanying manuscript (Foley et al., Submitted) shows that the splicing factor *psi* regulates *tim* alternative splicing in the same direction as when transferring the flies to colder temperatures. However, *psi* expression and activity are not modulated by temperature, suggesting that the temperature is sensed by a different system.

While *tim-cold* and *tim-M* are strongly post-transcriptionally regulated at all temperatures, the RISC binds also stronger to *tim-L* at 18°C. Indeed, *tim* has been reported to be regulated by miRNAs276a (Chen and Rosbash, 2016). Our miRNA-seq experiments suggest that miR-969 might be responsible for this temperature-specific regulation. However, it is possible that other miRNAs are involved and/or that other RNA binding proteins enhance the use of some miRNAs in a temperature-dependent way. CRISPR experiments targeting the miR-969 site could help distinguish between these possibilities. The miRNA profiling and AGO-IP experiments also suggest that other mRNAs might be regulated by miRNAs in a temperature-dependent way. It will be really interesting to match those datasets in order to understand how the transcriptional and post-transcriptional expression programs are regulated by temperature. Despite the large number of RNAs and miRNAs that are regulated in a temperature-dependent manner, the impact of temperature in alternative splicing seems to be quite restricted. Although we performed only a superficial analysis of the data, only *tim, per* and *Hsf* show evident temperature-dependent regulation of splicing (data not shown). Splicing is strongly temperature dependent, at least *in vitro*. Flies might have mechanisms that make the outcome of splicing temperature independent. This could be achieved by compensatory changes in chromatin structure, RNA pol II elongation rate or RNA editing which is known to be altered by temperature (Buchumenski et al., 2017). In addition, the specificity of the splicing strongly

549 suggests that the changes in *tim* splicing are unlikely to be due to the expression or activation
550 of a specific splicing factor. This possibility is supported by the findings reported in the
551 accompanying manuscript by Foley et al. showing that while *psi* regulates *tim* splicing, this
552 factor on its own cannot explain the temperature sensitivity of these alternative splicing events.
553 Importantly, our results demonstrate that the introns in isolation are still able to sense and
554 respond to the temperature changes (Figure 7). These results suggest that RNA structure
555 likely plays a key role in making this splicing events temperature sensitive. For example,
556 temperature could change the accessibility of *psi* binding sites in a temperature dependent
557 fashion. Interestingly, each temperature-driven splicing event might operate differently. For
558 example, production of *tim-sc* results from the competition between splicing and a cleavage
559 and polyadenylation event. On the other hand, production of *tim-M* and *tim-cold* depends on
560 an intron retention event. Interestingly, both introns have weak 3' splice sites but display
561 opposite temperature sensitivities, which suggest that their regulation depends on specific
562 structures and/or sequences and are not the results of general effects of temperature on
563 splicing.
564 We observed that flies that cannot generate *tim-sc* re-route *timeless* transcription towards the
565 other isoforms, mainly *tim-cold* (at both 18 and 25°C). These mutant flies also display altered
566 behavior. But what are the molecular actors responsible for these defects? *Tim-sc* mutant flies
567 display higher levels of *tim-cold* and *tim-L* at 25°C. It is difficult to rationalize how increased
568 levels of *tim-L* could trigger behavioral patterns observed in control flies at 18°C. We indeed
569 favor the possibility that the behavior observed in these flies at 25°C is due to increased
570 expression of *tim-cold* mRNA and protein. Previous work showed that TIM-COLD might act
571 differently than TIM-L (Montelli et al., 2015). Importantly, the increase in TIM-COLD protein in
572 the mutant flies might be significantly higher than the one on its RNA levels. This could happen
573 if for example, the increase in *tim-L* mRNA indirectly increases TIM-COLD levels by titrating
574 miR-969 or other miRNA targeting both to *tim-L* and *tim-cold* mRNAs. Additional CRISPR
575 mutants (i.e. abrogating *tim-cold* expression or making it constitutive) could help to completely
576 understand the mechanism behind this regulation.

577 Based on these and previous results we propose the following model in which miRNA-
578 mediated control imposes temperature-dependent thresholds for protein expression for the
579 different *tim* isoforms (Figure 8). At 25°C, *tim-L* and *tim-M* are produced. Both are moderately
580 regulated by miRNAs, due to sequences present in their last exon. *Tim-cold* production is low
581 at 25°C and the miRNA-mediated control is enough to abolish most (or all) protein expression
582 from this isoform at this temperature. In addition, *tim-M* is target of many additional miRNAs,
583 some of which are not differentially regulated by temperature, while others are higher at 29°C
584 or 18°C. Therefore, we predict that no TIM-M is produced at any temperature, and the
585 production of this isoform has a regulatory role (as recently suggested by Shakhmantsir et al.
586 (2018)). When the temperature is decreased, the strong increase in *tim-cold* overcomes
587 miRNA-mediated repression and some TIM-COLD is produced. In addition, *tim-sc* RNA and
588 protein are produced. We hypothesize that both TIM-COLD and TIM-SC contribute to the
589 phase advance and lower night activity observed at 18°C. TIM-SC lacks the cytoplasmic
590 retention domain and increased levels of this protein might lead to the phase advance
591 observed at 18°C. At 29°C, *Tim-M* is increased but TIM amounts are maintained constant
592 likely due to higher production rates of TIM (due to a more modest association of *tim-L* with
593 AGO1). In this way, *tim* co and post-transcriptional regulation can modulate the amounts and
594 type of TIM proteins to facilitate temperature adaptation. It is possible that these changes in
595 alternative splicing could regulate other situations in which the circadian clock requires
596 adjustments of TIM levels and/or activity independently of CLK-driven transcription. These
597 could include entrainment by temperature or light as well as cell to cell synchronization.
598 Moreover, as *tim* is being alternatively spliced, it is even possible that some of these protein
599 isoforms could be used by the cell as temperature sensors.
600 In sum, in this study we determine that *tim* is extensively regulated by alternative splicing in a
601 temperature dependent way. Moreover, we show that this regulation is, at least partially,
602 responsible for temperature adaptation. We propose that this complex regulation of alternative
603 splicing and miRNA-mediated control provides a mechanism for altering the relationship
604 between TIM and PER proteins. This would allow the modulation of the circadian phase

without affecting the period (which is strongly dependent on CLK and PER protein levels and activity). Last but not least, our data suggest that *tim* alternative splicing might act as a thermometer for the cell and might regulate temperature responses not related to the circadian clock.

ACKNOWLEDGMENTS:

We thank Avigayel Rabin and Reut Ashwall-Fluss for help with the alignment of the RNA seq data. This work was funded by the Binational Foundation (BSF Transformative Program), the ISF Legacy Program (Morasha, #1649/16) and the iCoreI-CORE Program of the Planning and Budgeting Committee in Israel (1796/12). All the RNA-seq data has been submitted to GEO (entries GSE124134, 124135, 124141, 123142, 124200 and 124201).

AUTHOR CONTRIBUTIONS:

NE generated the plasmids, performed the cell culture experiments and generate the CRISPR flies. AMA performed the behavioral analysis as well as the qRT-PCRs, analyzed the data, generated the figures and wrote the manuscript. OB generated the RNA-seq libraries, AGO-IP experiments and western blots. ILP performed the computational analysis. RW performed the behavioral experiments in the non-melanogaster *Drosophila* species. SK designed the experiments and wrote the manuscript.

DECLARATION OF INTEREST:

The authors declare no competing interests.

Materials and Methods

Fly husbandry

Drosophila yakuba, *Drosophila simulans* and *Drosophila virilis* were obtained from the Drosophila Species Stock Center (DSSC) at the University of California, San Diego. CantonS flies were used as wild type strain for *Drosophila melanogaster*. Additionally, tim^{0} and per^{01} strains have been described previously in (Konopka and Benzer, 1971; Sehgal et al., 1994). Transgenic lines for the overexpression of different FLAG-tagged *tim* isoforms or luciferase fused to their 3'UTRs were generated by injecting the plasmids (described below) in a site-specific manner into the pattP2 site using the PhiC31 integrase-mediated transgenesis system (Best Gene Drosophila Embryo Injection Services). These transgenic flies were crossed to *tim-Gal4* driver (Blau and Young, 1999; Kaneko and Hall, 2000).

All crosses were performed and raised at 25°C. Newborn adults were either maintained at 25°C or switched to colder (18°C) or warmer (29°C) temperatures as described in the text.

Generation of *tim-sc* polyadenylation and cleavage signal mutants by CRISPR

The *tim-sc* mutant flies were generated following the protocol from Ge et al. (2016) with some modifications. pCFD5 plasmid (Addgene, plasmid #73914) was modified to exclude *Vermilion* and *attB* (pCFD5d). 3 gRNAs (one targeting *w* gene and two, *tim*) were generated from PCR templates and cloned intro pCFD5d (pCFD5d*w/tim*-1,2) as described in (Fu et al., 2014; Port and Bullock, 2016; Port et al., 2014). The donor template for homologous recombination contained a point mutation in an intronic sequence as well as a silent point mutation (one in each site targeted by the gRNAs). This fragment was then cloned into pUC57-*white*[coffee] (Addgene, plasmid #84006) between the SacI and HindIII sites (pUC57-*timShort*).

pCFD5d*w/tim*-1,2, pUC57-*white*[coffee] and pUC57-*timShort* were injected into *vas-Cas9* (y^{1}, *M(Ferguson et al.)ZH-2A*) flies (Ge et al., 2016) by Rainbow Transgenic Flies, Inc. (Camarillo, CA). G0 flies were crossed to second chromosome balancers and individual G1 *Cyo* flies from non-red-eyed populations were again mated to the 2nd chr balancers. Individual G1 flies were

subsequently genotyped to verify the deletion and the possibility of random integration either in the genome or at CAS9 cutting sites of the plasmid was assessed as described in (Ge et al., 2016). G2 *cyo* male and female flies from positive crosses were crossed to obtain non *cyo* homozygous stocks. Finally, the entire *tim* locus was sequenced in the *tim-sc* mutants and their isogenic controls to verify that there were no additional mutations in the *tim* locus.

Plasmids for S2 cells transfection and/or injection into *Drosophila*

pMT-*Clk* was previously described in (Weiss et al., 2014) and p-Act-Gal4 (Addgene, plasmid #24344).

C-terminus FLAG-tagged UAS-*tim* overexpression plasmids

cDNA from Canton-S heads of flies reared at 18 (for *tim-sc* and *tim-cold*), 25 (*tim-L*) or 29°C (*tim-M*) were used to amplify each isoform. NotI and KpnI restriction sites and a FLAG-tag sequence (at the 3' of the coding DNA but before the stop codon) were added by PCR. Each isoform was finally cloned into the pUASTattB vector between the NotI and KpnI sites.

UAS-*luciferase-3'UTR* of each *tim* isoform plasmids

A PCR product containing the *Firefly Luciferase* gene was cloned into pUASTattB (pUAST-*luc*-attB). The 3' UTRs of all four isoforms were amplified from fly head cDNA and cloned into the pUAST-*luc*-attB vector between NotI and XhoI sites.

tim exon-intron-exon minigenes

A plasmid containing exon5-intron5-exon6 (*tim-control*), exon10-intron10-exon11 (*tim-sc*), exon13-intron13-exon14 (*tim-M*) and exon16-intron16-exon17 (*tim-cold*) fragments defined by KpnI and XhoI restriction sites was ordered from Syntezza Bioscience Ltd. This plasmid was then cut with KpnI and XhoI. The four fragments were extracted and cloned into pMT-V5 (Invitrogen).

Cell culture and transfections

Drosophila Schneider-2 (S2) cells were cultured in 10% fetal bovine serum (Invitrogen) insect tissue culture medium (Biological industries) as in (Weiss et al., 2014). The experiments were performed at 18°C or 25°C, as described in the text.

Luciferase activity assay

Luciferase activity from S2 cells was measured using the Dual Luciferase Assay Kit (Promega) following the manufacturer's instructions as in (Krishnan et al., 2001; Weiss et al., 2014). Luciferase measurements from fly wings was performed as previously described (Plautz and Kay, 1999).

RNA libraries preparation for RNA-seq

DGE (3'end-seq)

Flies were entrained for at least 3 days at 18°C, 25°C or 29°C and collected at 6 different timepoints (ZT3, ZT7, ZT11, ZT15, ZT19 and ZT23). RNA from the fly heads was extracted using TRIzol reagent (SIGMA). 3'-seq libraries were prepared as previously described (Shishki et al., Afik et al., 2017). These data have been deposited at NCBI GEO as XXX.

Total RNA-seq

RNA from fly heads collected at two or three different timepoints (ZT 3, 15 and 21 for 18C and 29C and ZT3 and 15 for 25C) was extracted using Trizol and used to generate polyA+ RNA-seq libraries. The library preparation procedure was modified from (Engreitz et al., 2013) as follows: 0.5µg of total RNA was polyA+ selected (using Oligo(dT) beads, Invitrogen), fragmented in FastAP buffer (Thermo Scientific) for 3min at 940 C, then dephosphorylated with FastAP, cleaned (using SPRI beads, Agencourt) and ligated to a linker1 (5Phos/AXXXXXXXXAGATCGGAAGAGCGTCGTGTAG/3ddC/, where XXXXXXXX is an internal barcode specific for each sample), using T4 RNA ligase I (NEB). Ligated RNA was cleaned-up with Silane beads (Dynabeads MyOne, Life Technologies) and pooled into a single tube. RT was then performed for the pooled sample, with a specific primer (5´-CCTACACGACGCTCTTCC-3´) using AffinityScript Multiple Temperature cDNA Synthesis Kit

(Agilent Technologies). Then, RNA-DNA hybrids were degraded by incubating the RT mixture with 10% 1M NaOH (e.g. 2ul to 20ul of RT mixture) at 700 C for 12 minutes. pH was then normalized by addition of corresponding amount of 0.5M AcOH (e.g. 4ul for 22 ul of NaOH+RT mixture). The reaction mixture was cleaned up using Silane beads and second ligation was performed, where 3'end of cDNA was ligated to linker2 (5Phos/AGATCGGAAGAGCACACGTCTG/3ddC/) using T4 RNA ligase I. The sequences of linker1 and linker2 are partially complementary to the standard Illumina read1 and read2/barcode adapters, respectively. Reaction Mixture was cleaned up (Silane beads) and PCR enrichment was set up using enrichment primers 1 and 2: (5'AATGATACGGCGACCACCGAGATCTACACTCTTTCCCTACACGACGCTCTTCCGA TCT-3', 5'-CAAGCAGAAGACGGCATACGAGATXXXXXXXXGTGACTGGAGTTCAGAC GTGTGCTCTTCCGATCT-3', where XXXXXXX is barcode sequence) and Phusion HF MasterMix (NEB). 12 cycles of enrichment were performed. Libraries were cleaned with 0.7X volume of SPRI beads. Libraries were characterization by Tapestation. RNA was sequenced as paired-end samples, in a NextSeq 500 sequencer (Illumina).

AGO1-IP followed by small RNA sequencing

The samples were collected at 18°C, 25°C or 29°C at four different timepoints (ZT3, ZT9, ZT15 and ZT21). AGO1 immunoprecipitation was performed as previously described (Kadener et al., 2009; Lerner et al., 2015). The small RNA libraries were constructed using NEBNext® Small RNA Laibrary Prep Set for Illumina.

AGO1-IP followed by Oligonucleotide microarrays

The samples were collected at 18°C, 25°C or 29°C. AGO1 immunoprecipitation was performed as previously described (Kadener et al., 2009; Lerner et al., 2015). INPUT and AGO IP Total RNA was extracted from fly heads using TRI reagent (Sigma) according to manufacturer's protocol. cDNA synthesis was carried out as described in the Expression Analysis Technical Manual (Affymetrix). The cRNA reactions were carried out using the IVT

kit (Affymetrix). Affymetrix high-density arrays for Drosophila melanogaster version 2.0 were probed, hybridized, stained, and washed according to the manufacturer's protocol.

Microarray Analysis*:*

The R Bioconductor affy package (http://www.bioconductor.org) was used to normalize and calculate summary values from Affymetrix CEL files using gcRMA (Bioconductor). Gene ontology enrichment analysis was performed as described in Mezan et al. (2013). To determine AGO-IP enrichment ranking, we ranked the residuals from a linear model was between the normalized reads in the IP and the INPUT.

RNA seq analysis.

The total RNA sequencing reads were aligned to the *Drosophila melanogaster* genome version dm3. For the different species, alternative splicing proportion was calculated manually searching the exon-exon junction.

For the small RNA sequencing, the reads were processed using miRExpress pipeline (Wang et al., 2009) using miRBase 21 version. The different circadian timepoints were considered independent replicates (n=4) and the differential gene expression analysis was done using a negative binomial model using DeSeq2 package on R. A miRNA with p adjusted value less than 0.05 and an absolute log2(fold change) more than 1 was considered differentially expressed.

For the DGE data, the circadian analysis was performed using the package MetaCycle (Wu et al., 2016). For each temperature and circadian timepoint, two replicates were analyzed (n=2). To normalize over different library preparation, after normalizing by library size the counts were divided by the maximum in each replicate. Genes with more than two cero counts in any timepoint was discarded from further analysis. The amplitude for each replicate was then calculated as the maximum divided the minimum for each gene. JTK algorithm was used for the circadian analysis. A gene was considered as cycling if the JTK pvalue was less than

0.05 and the amplitude was more than 1.5. For these genes, the phase shift was calculated as the phase at 25ºC minus the phase at 18ºC or 29ºC.

TargetScan analysis of putative miRNA binding to each *tim* 3'UTR

As not all of the 3'UTRs for the different *tim* isoforms are annotated, TargetScanFly version 6.1 was run locally (which allows manual entry of the sequences of interest). UTR sequences were downloaded from UCSC dm6 27way conservation. This way we identified several putative miRNAs binding to each of the isoforms. We continued by manually looking at the abundance of this miRNAs (from the AGO1-IP followed by smallRNA sequencing) in order to determine which of those putative miRNAs are being expressed in the fly heads. Additionally, we defined as miRNAs that change in a temperature-dependent manner those miRNAs that had more than 2-fold change between 18 and 29°C and in which this difference was statistically significant (pval<0.05).

Chromatin-bound (nascent) RNA

Performed as described in (Lerner et al., 2015).

Real Time PCR analysis

Total RNA was extracted from adult fly heads (or brains) at the mentioned timepoints using TRI Reagent (Sigma) and treated with DNase I (NEB) following the manufacturer's protocol. cDNA was synthesized from this RNA (using iScript and oligodT primers, Bio-Rad) and diluted 1:60 prior to performing the quantitative real-time PCR using SYBR green (Bio-Rad) in a C1000 Thermal Cycler Bio-Rad. Primers used for amplifying each isoform were: *tim*-sc (5'-AACACAACCAGGAGCATAC -3' and 5'- ATGGTCCACAAATGTTAAAA -3'), *tim*-M (5'-GGAGACAATGTACGGACTC -3' and 5'- ATTTCACACAGAGAGAGAGC -3'), *tim*-cold (5'-GCATCTGTGTACGAAAAGGA -3' and 5'- ATGTAACCTATGTGCGACTC -3'), *tim-L* and *tim*-M (5'- CTCCATGAAGTCCTCGTTC -3' and 5'- TGTCGCTGTTTAATTCCTTC -3') and

824 junction between exons 5-6 which are present in all isoforms (5'-
825 AAAAGCAGCCTCATCAACAT -3' and 5'- AGATAGCTGTAACCCTTGAG -3').
826 The PCR mixture was subjected to 95 °C for 3 min, followed by 40 cycles of 95 °C for 10 s,
827 55 °C for 10 s and 72 °C for 30 s followed by a melting curve analysis. Fluorescence intensities
828 were plotted versus the number of cycles by using an algorithm provided by the manufacturer
829 (CFX Maestro Software, Bio-Rad). The results were normalized against *rp49* (5'-
830 TACAGGCCCAAGATCGTGAA -3' and 5'- CCATTTGTGCGACAGCTTAG -3') and *tub* (5'-
831 TGCTCACGAAAAGCTCTCCT -3' and 5'- CACACACGCACTATCAGCAA -3') levels.
832
833 **Western blotting**
834 Protein was extracted from fly heads and WB performed as in (Weiss et al., 2014). Antibodies
835 used: rat anti-TIM (1:30,000, a kind gift from Michael Rosbash), mouse anti-FLAG-M2
836 (1:20,000; Sigma F3165) and mouse anti-Tub (1:20,000, DM1A, SIGMA). Quantifications
837 were done utilizing Image J software.
838
839 **Assessment of the locomotor behavior**
840 Male flies were placed into a glass tube containing 2% agarose and 5% sucrose food and their
841 activity was monitored using Trikinetics *Drosophila* Activity Monitors (Waltham, MA, USA).
842 Flies were maintained for 4 days in 12:12 Light: Dark cycles (LD) and 5 days in constant
843 darkness (DD). The experiments were performed at 18, 25 or 29°C, as indicated. Analyses
844 were performed with a signal processing toolbox (Levine et al., 2002).
845 All the activity assessments were done in LD. For the calculation of the beginning of the
846 evening peak, the activity of flies were analyzed individually on 30-minutes intervals. The
847 criteria were: (1) have a trend of increasing activity, (2) no more than 1/3 of the bins can be
848 outliers and (3) a reduction of less than 10% of the activity was not counted as an outlier. Only
849 flies in which an evening peak was clearly distinguishable were included in this analysis.
850
851

852 **REFERENCES**

853 Afik, S., O. Bartok, M. N. Artyomov, A. A. Shishkin, S. Kadri, M. Hanan, X. Zhu, M. Garber, and S.
854 Kadener, 2017, Defining the 5 and 3 landscape of the Drosophila transcriptome with Exo-seq
855 and RNaseH-seq: Nucleic Acids Res, v. 45, p. e95.
856 Allada, R., and B. Y. Chung, 2010, Circadian organization of behavior and physiology in Drosophila:
857 Annu Rev Physiol, v. 72, p. 605-24.
858 Anders, S., A. Reyes, and W. Huber, 2012, Detecting differential usage of exons from RNA-seq data:
859 Genome Res, v. 22, p. 2008-17.
860 Baralle, F. E., and J. Giudice, 2017, Alternative splicing as a regulator of development and tissue
861 identity: Nat Rev Mol Cell Biol, v. 18, p. 437-451.
862 Bartok, O., C. P. Kyriacou, J. Levine, A. Sehgal, and S. Kadener, 2013, Adaptation of molecular
863 circadian clockwork to environmental changes: a role for alternative splicing and miRNAs:
864 Proc Biol Sci, v. 280, p. 20130011.
865 Blau, J., and M. W. Young, 1999, Cycling *vrille* expression is required for a functional *Drosophila*
866 clock: Cell, v. 99, p. 661-71.
867 Boothroyd, C. E., H. Wijnen, F. Naef, L. Saez, and M. W. Young, 2007a, Integration of light and
868 temperature in the regulation of circadian gene expression in Drosophila: Plos Genetics, v. 3.
869 Boothroyd, C. E., H. Wijnen, F. Naef, L. Saez, and M. W. Young, 2007b, Integration of light and
870 temperature in the regulation of circadian gene expression in Drosophila: PLoS Genet, v. 3.
871 Buchumenski, I., O. Bartok, R. Ashwal-Fluss, V. Pandey, H. T. Porath, E. Y. Levanon, and S. Kadener,
872 2017, Dynamic hyper-editing underlies temperature adaptation in Drosophila: PLoS Genet, v.
873 13, p. e1006931.
874 Caceres, J. F., and A. R. Kornblihtt, 2002, Alternative splicing: multiple control mechanisms and
875 involvement in human disease: Trends Genet, v. 18, p. 186-93.
876 Chen, X., and M. Rosbash, 2016, *mir-276a* strengthens *Drosophila* circadian rhythms by regulating
877 *timeless* expression: Proc Natl Acad Sci U S A, v. 113, p. E2965-72.
878 Collins, B. H., E. Rosato, and C. P. Kyriacou, 2004, Seasonal behavior in Drosophila melanogaster
879 requires the photoreceptors, the circadian clock, and phospholipase C: Proc Natl Acad Sci U S
880 A, v. 101, p. 1945-50.
881 de la Mata, M., C. R. Alonso, S. Kadener, J. P. Fededa, M. Blaustein, F. Pelisch, P. Cramer, D. Bentley,
882 and A. R. Kornblihtt, 2003, A slow RNA polymerase II affects alternative splicing in vivo: Mol
883 Cell, v. 12, p. 525-32.
884 Derr, A., C. Yang, R. Zilionis, A. Sergushichev, D. M. Blodgett, S. Redick, R. Bortell, J. Luban, D. M.
885 Harlan, S. Kadener, D. L. Greiner, A. Klein, M. N. Artyomov, and M. Garber, 2016, End
886 Sequence Analysis Toolkit (ESAT) expands the extractable information from single-cell RNA-
887 seq data: Genome Res, v. 26, p. 1397-1410.
888 Dissel, S., C. N. Hansen, O. Ozkaya, M. Hemsley, C. P. Kyriacou, and E. Rosato, 2014, The logic of
889 circadian organization in *Drosophila*: Curr Biol, v. 24, p. 2257-66.
890 Dobin, A., C. A. Davis, F. Schlesinger, J. Drenkow, C. Zaleski, S. Jha, P. Batut, M. Chaisson, and T. R.
891 Gingeras, 2013, STAR: ultrafast universal RNA-seq aligner: Bioinformatics, v. 29, p. 15-21.
892 Emery, P., W. V. So, M. Kaneko, J. C. Hall, and M. Rosbash, 1998, CRY, a Drosophila clock and light-
893 regulated cryptochrome, is a major contributor to circadian rhythm resetting and
894 photosensitivity: Cell, v. 95, p. 669-79.
895 Fathallah-Shaykh, H. M., J. L. Bona, and S. Kadener, 2009, Mathematical model of the Drosophila
896 circadian clock: loop regulation and transcriptional integration: Biophys J, v. 97, p. 2399-408.
897 Ferguson, S. B., M. A. Blundon, M. S. Klovstad, and T. Schupbach, 2012, Modulation of *gurken*
898 translation by insulin and TOR signaling in *Drosophila*: J Cell Sci, v. 125, p. 1407-19.
899 Foley, L., J. Ling, N. Evantalm, S. Kadener, and P. Emery, Submitted, PSI controls *tim* splicing and
900 circadian period in *Drosophila*.
901 Fu, Y., J. D. Sander, D. Reyon, V. M. Cascio, and J. K. Joung, 2014, Improving CRISPR-Cas nuclease
902 specificity using truncated guide RNAs: Nat Biotechnol, v. 32, p. 279-284.

Ge, D. T., C. Tipping, M. H. Brodsky, and P. D. Zamore, 2016, Rapid Screening for CRISPR-Directed Editing of the Drosophila Genome Using white Coconversion: G3 (Bethesda), v. 6, p. 3197-3206.

Glaser, F. T., and R. Stanewsky, 2005, Temperature synchronization of the Drosophila circadian clock: Curr Biol, v. 15, p. 1352-63.

Grima, B., E. Chelot, R. Xia, and F. Rouyer, 2004, Morning and evening peaks of activity rely on different clock neurons of the Drosophila brain: Nature, v. 431, p. 869-73.

Hall, J. C., 2003, Genetics and molecular biology of rhythms in Drosophila and other insects: Adv Genet, v. 48, p. 1-280.

Hardin, P. E., 2011, Molecular genetic analysis of circadian timekeeping in Drosophila: Adv Genet, v. 74, p. 141-73.

Hardin, P. E., and S. Panda, 2013, Circadian timekeeping and output mechanisms in animals: Curr Opin Neurobiol, v. 23, p. 724-31.

Harms, E., S. Kivimae, M. W. Young, and L. Saez, 2004, Posttranscriptional and posttranslational regulation of clock genes: J Biol Rhythms, v. 19, p. 361-73.

Helfrich-Forster, C., 2003, The neuroarchitecture of the circadian clock in the brain of Drosophila melanogaster: Microsc Res Tech, v. 62, p. 94-102.

Im, S. H., W. Li, and P. H. Taghert, 2011, PDFR and CRY signaling converge in a subset of clock neurons to modulate the amplitude and phase of circadian behavior in Drosophila: PLoS One, v. 6, p. e18974.

Ito, C., S. G. Goto, K. Tomioka, and H. Numata, 2011, Temperature Entrainment of the Circadian Cuticle Deposition Rhythm in Drosophila melanogaster: J Biol Rhythms, v. 26, p. 14-23.

Jan, L. Y., and Y. N. Jan, 1976, Properties of the larval neuromuscular junction in Drosophila melanogaster: J Physiol, v. 262, p. 189-214.

Kadener, S., J. S. Menet, R. Schoer, and M. Rosbash, 2008, Circadian transcription contributes to core period determination in Drosophila: PLoS Biol, v. 6, p. e119.

Kadener, S., J. S. Menet, K. Sugino, M. D. Horwich, U. Weissbein, P. Nawathean, V. V. Vagin, P. D. Zamore, S. B. Nelson, and M. Rosbash, 2009, A role for microRNAs in the Drosophila circadian clock: Genes Dev, v. 23, p. 2179-91.

Kaneko, M., and J. C. Hall, 2000, Neuroanatomy of cells expressing clock genes in *Drosophila*: transgenic manipulation of the *period* and *timeless* genes to mark the perikarya of circadian pacemaker neurons and their projections: J Comp Neurol, v. 422, p. 66-94.

Kidd, P. B., M. W. Young, and E. D. Siggia, 2015, Temperature compensation and temperature sensation in the circadian clock: Proc Natl Acad Sci U S A, v. 112, p. E6284-92.

Ko, W. Y., R. M. David, and H. Akashi, 2003, Molecular phylogeny of the Drosophila melanogaster species subgroup: J Mol Evol, v. 57, p. 562-73.

Koh, K., X. Zheng, and A. Sehgal, 2006, JETLAG resets the Drosophila circadian clock by promoting light-induced degradation of TIMELESS: Science, v. 312, p. 1809-12.

Kojima, S., D. L. Shingle, and C. B. Green, 2011, Post-transcriptional control of circadian rhythms: J Cell Sci, v. 124, p. 311-20.

Konopka, R. J., and S. Benzer, 1971, Clock mutants of *Drosophila melanogaster*: Proc Natl Acad Sci U S A, v. 68, p. 2112-6.

Krishnan, B., J. D. Levine, M. K. Lynch, H. B. Dowse, P. Funes, J. C. Hall, P. E. Hardin, and S. E. Dryer, 2001, A new role for cryptochrome in a Drosophila circadian oscillator: Nature, v. 411, p. 313-7.

Kuntz, S. G., and M. B. Eisen, 2014, Drosophila embryogenesis scales uniformly across temperature in developmentally diverse species: PLoS Genet, v. 10, p. e1004293.

Kuromi, H., and Y. Kidokoro, 1999, The optically determined size of exo/endo cycling vesicle pool correlates with the quantal content at the neuromuscular junction of Drosophila larvae: J Neurosci, v. 19, p. 1557-65.

953 Lerner, I., O. Bartok, V. Wolfson, J. S. Menet, U. Weissbein, S. Afik, D. Haimovich, C. Gafni, N.
954 Friedman, M. Rosbash, and S. Kadener, 2015, Clk post-transcriptional control denoises
955 circadian transcription both temporally and spatially: Nat Commun, v. 6, p. 7056.
956 Levine, J. D., P. Funes, H. B. Dowse, and J. C. Hall, 2002, Signal analysis of behavioral and molecular
957 cycles: BMC Neurosci, v. 3, p. 1.
958 Li, Y., F. Guo, J. Shen, and M. Rosbash, 2014, PDF and cAMP enhance PER stability in Drosophila clock
959 neurons: Proc Natl Acad Sci U S A, v. 111, p. E1284-90.
960 Lim, C., and R. Allada, 2013, Emerging roles for post-transcriptional regulation in circadian clocks:
961 Nat Neurosci, v. 16, p. 1544-50.
962 Lin, F. J., W. Song, E. Meyer-Bernstein, N. Naidoo, and A. Sehgal, 2001, Photic signaling by
963 cryptochrome in the Drosophila circadian system: Mol Cell Biol, v. 21, p. 7287-94.
964 Love, M. I., W. Huber, and S. Anders, 2014, Moderated estimation of fold change and dispersion for
965 RNA-seq data with DESeq2: Genome Biol, v. 15, p. 550.
966 Low, K. H., C. Lim, H. W. Ko, and I. Edery, 2008, Natural variation in the splice site strength of a clock
967 gene and species-specific thermal adaptation: Neuron, v. 60, p. 1054-67.
968 Majercak, J., D. Sidote, P. E. Hardin, and I. Edery, 1999, How a circadian clock adapts to seasonal
969 decreases in temperature and day length: Neuron, v. 24, p. 219-30.
970 Markow, T. A., and P. M. O'Grady, 2007, Drosophila biology in the genomic age: Genetics, v. 177, p.
971 1269-76.
972 Memczak, S., M. Jens, A. Elefsinioti, F. Torti, J. Krueger, A. Rybak, L. Maier, S. D. Mackowiak, L. H.
973 Gregersen, M. Munschauer, A. Loewer, U. Ziebold, M. Landthaler, C. Kocks, F. le Noble, and
974 N. Rajewsky, 2013, Circular RNAs are a large class of animal RNAs with regulatory potency:
975 Nature, v. 495, p. 333-8.
976 Mezan, S., R. Ashwal-Fluss, R. Shenhav, M. Garber, and S. Kadener, 2013, Genome-wide assessment
977 of post-transcriptional control in the fly brain: Front Mol Neurosci, v. 6, p. 49.
978 Mezan, S., J. D. Feuz, B. Deplancke, and S. Kadener, 2016, PDF Signaling Is an Integral Part of the
979 Drosophila Circadian Molecular Oscillator: Cell Rep, v. 17, p. 708-719.
980 Myers, M. P., K. Wager-Smith, C. S. Wesley, M. W. Young, and A. Sehgal, 1995, Positional cloning and
981 sequence analysis of the Drosophila clock gene, timeless: Science, v. 270, p. 805-8.
982 Ogueta, M., R. C. Hardie, and R. Stanewsky, 2018, Non-canonical Phototransduction Mediates
983 Synchronization of the Drosophila melanogaster Circadian Clock and Retinal Light
984 Responses: Curr Biol, v. 28, p. 1725-1735 e3.
985 Ozkaya, O., and E. Rosato, 2012, The circadian clock of the fly: a neurogenetics journey through time:
986 Adv Genet, v. 77, p. 79-123.
987 Pamudurti, N. R., O. Bartok, M. Jens, R. Ashwal-Fluss, C. Stottmeister, L. Ruhe, M. Hanan, E. Wyler, D.
988 Perez-Hernandez, E. Ramberger, S. Shenzis, M. Samson, G. Dittmar, M. Landthaler, M.
989 Chekulaeva, N. Rajewsky, and S. Kadener, 2017, Translation of CircRNAs: Mol Cell, v. 66, p. 9-
990 21 e7.
991 Peng, Y., D. Stoleru, J. D. Levine, J. C. Hall, and M. Rosbash, 2003, Drosophila free-running rhythms
992 require intercellular communication: PLoS Biol, v. 1, p. E13.
993 Petrillo, E., S. E. Sanchez, A. R. Kornblihtt, and M. J. Yanovsky, 2011, Alternative splicing adds a new
994 loop to the circadian clock: Commun Integr Biol, v. 4, p. 284-286.
995 Pilorz, V., C. Helfrich-Förster, and H. Oster, 2018, The role of the circadian clock system in physiology:
996 Pflügers Archiv - European Journal of Physiology, v. 470, p. 227-239.
997 Plautz, J. D., and S. A. Kay, 1999, Synchronous real-time reporting of multiple cellular events:
998 Methods Cell Biol, v. 58, p. 283-91.
999 Port, F., and S. L. Bullock, 2016, Augmenting CRISPR applications in Drosophila with tRNA-flanked
1000 sgRNAs: Nat Methods, v. 13, p. 852-4.
1001 Port, F., H. M. Chen, T. Lee, and S. L. Bullock, 2014, Optimized CRISPR/Cas tools for efficient germline
1002 and somatic genome engineering in Drosophila: Proc Natl Acad Sci U S A, v. 111, p. E2967-
1003 76.

Reese, M. G., F. H. Eeckman, D. Kulp, and D. Haussler, 1997, Improved splice site detection in Genie: J Comput Biol, v. 4, p. 311-23.

Roessingh, S., W. Wolfgang, and R. Stanewsky, 2015, Loss of *Drosophila melanogaster* TRPA1 Function Affects "Siesta" Behavior but Not Synchronization to Temperature Cycles: J Biol Rhythms, v. 30, p. 492-505.

Rothenfluh, A., M. Abodeely, J. L. Price, and M. W. Young, 2000, Isolation and analysis of six timeless alleles that cause short- or long-period circadian rhythms in Drosophila: Genetics, v. 156, p. 665-75.

Russo, C. A., N. Takezaki, and M. Nei, 1995, Molecular phylogeny and divergence times of drosophilid species: Mol Biol Evol, v. 12, p. 391-404.

Sanchez, S. E., E. Petrillo, E. J. Beckwith, X. Zhang, M. L. Rugnone, C. E. Hernando, J. C. Cuevas, M. A. Godoy Herz, A. Depetris-Chauvin, C. G. Simpson, J. W. Brown, P. D. Cerdan, J. O. Borevitz, P. Mas, M. F. Ceriani, A. R. Kornblihtt, and M. J. Yanovsky, 2010, A methyl transferase links the circadian clock to the regulation of alternative splicing: Nature, v. 468, p. 112-6.

Sanchez, S. E., E. Petrillo, A. R. Kornblihtt, and M. J. Yanovsky, 2011, Alternative splicing at the right time: RNA Biol, v. 8, p. 954-9.

Schlichting, M., P. Menegazzi, K. R. Lelito, Z. Yao, E. Buhl, E. Dalla Benetta, A. Bahle, J. Denike, J. J. Hodge, C. Helfrich-Forster, and O. T. Shafer, 2016, A Neural Network Underlying Circadian Entrainment and Photoperiodic Adjustment of Sleep and Activity in *Drosophila*: J Neurosci, v. 36, p. 9084-96.

Sehgal, A., J. L. Price, B. Man, and M. W. Young, 1994, Loss of circadian behavioral rhythms and *per* RNA oscillations in the *Drosophila* mutant *timeless*: Science, v. 263, p. 1603-6.

Seluzicki, A., M. Flourakis, E. Kula-Eversole, L. Zhang, V. Kilman, and R. Allada, 2014, Dual PDF signaling pathways reset clocks via TIMELESS and acutely excite target neurons to control circadian behavior: PLoS Biol, v. 12, p. e1001810.

Shafer, O. T., C. Helfrich-Forster, S. C. Renn, and P. H. Taghert, 2006, Reevaluation of *Drosophila melanogaster*'s neuronal circadian pacemakers reveals new neuronal classes: J Comp Neurol, v. 498, p. 180-93.

Shakhmantsir, I., S. Nayak, G. R. Grant, and A. Sehgal, 2018, Spliceosome factors target timeless (tim) mRNA to control clock protein accumulation and circadian behavior in Drosophila: Elife, v. 7.

Stoleru, D., Y. Peng, J. Agosto, and M. Rosbash, 2004, Coupled oscillators control morning and evening locomotor behaviour of Drosophila: Nature, v. 431, p. 862-8.

Stoleru, D., Y. Peng, P. Nawathean, and M. Rosbash, 2005, A resetting signal between Drosophila pacemakers synchronizes morning and evening activity: Nature, v. 438, p. 238-42.

Taghert, P. H., and O. T. Shafer, 2006, Mechanisms of clock output in the *Drosophila* circadian pacemaker system: J Biol Rhythms, v. 21, p. 445-57.

Trapnell, C., L. Pachter, and S. L. Salzberg, 2009, TopHat: discovering splice junctions with RNA-Seq: Bioinformatics, v. 25, p. 1105-11.

van Dongen, S., C. Abreu-Goodger, and A. J. Enright, 2008, Detecting microRNA binding and siRNA off-target effects from expression data: Nat Methods, v. 5, p. 1023-5.

Wang, Q., K. C. Abruzzi, M. Rosbash, and D. C. Rio, 2018, Striking circadian neuron diversity and cycling of Drosophila alternative splicing: Elife, v. 7.

Wang, W. C., F. M. Lin, W. C. Chang, K. Y. Lin, H. D. Huang, and N. S. Lin, 2009, miRExpress: analyzing high-throughput sequencing data for profiling microRNA expression: BMC Bioinformatics, v. 10, p. 328.

Weiss, R., O. Bartok, S. Mezan, Y. Malka, and S. Kadener, 2014, Synergistic interactions between the molecular and neuronal circadian networks drive robust behavioral circadian rhythms in Drosophila melanogaster: PLoS Genet, v. 10, p. e1004252.

Westholm, J. O., P. Miura, S. Olson, S. Shenker, B. Joseph, P. Sanfilippo, S. E. Celniker, B. R. Graveley, and E. C. Lai, 2014, Genome-wide analysis of drosophila circular RNAs reveals their structural and sequence properties and age-dependent neural accumulation: Cell Rep, v. 9, p. 1966-80.

Wijnen, H., F. Naef, C. Boothroyd, A. Claridge-Chang, and M. W. Young, 2006, Control of daily transcript oscillations in Drosophila by light and the circadian clock: Plos Genetics, v. 2, p. 326-343.

Wolfgang, W., A. Simoni, C. Gentile, and R. Stanewsky, 2013, The Pyrexia transient receptor potential channel mediates circadian clock synchronization to low temperature cycles in Drosophila melanogaster: Proc Biol Sci, v. 280, p. 20130959.

Wu, G., R. C. Anafi, M. E. Hughes, K. Kornacker, and J. B. Hogenesch, 2016, MetaCycle: an integrated R package to evaluate periodicity in large scale data: Bioinformatics, v. 32, p. 3351-3353.

Xue, Y., and Y. Zhang, 2018, Emerging roles for microRNA in the regulation of *Drosophila* circadian clock: BMC Neurosci, v. 19, p. 1.

Yang, Z., and A. Sehgal, 2001, Role of molecular oscillations in generating behavioral rhythms in Drosophila: Neuron, v. 29, p. 453-67.

Yoshii, T., D. Rieger, and C. Helfrich-Forster, 2012, Two clocks in the brain: an update of the morning and evening oscillator model in *Drosophila*: Prog Brain Res, v. 199, p. 59-82.

Yu, W., H. Zheng, J. H. Houl, B. Dauwalder, and P. E. Hardin, 2006, PER-dependent rhythms in CLK phosphorylation and E-box binding regulate circadian transcription: Genes Dev, v. 20, p. 723-33.

Zhou J, Y. W., Hardin PE, 2016, CLOCKWORK ORANGE Enhances PERIOD Mediated Rhythms in Transcriptional Repression by Antagonizing E-box Binding by CLOCK-CYCLE: PLOS Genetics, v. 12(11): e1006430.

Figure Legends

Figure 1. Temperature remodels the circadian transcriptome. A. Heat maps of normalized gene expression for genes that display 24hs cycling expression at different temperatures. Flies were entrained at the indicated temperatures for 3 days in 12:12 Light: Dark (LD) conditions. Fly heads were collected every 4 hours in 12 independent timepoints. Cycling expression was assessed as indicated in material and methods. **B.** Venn diagrams indicating the number of oscillating genes at different temperatures. **C.** Density plot showing the phases of core clock genes cycling at both 18°C and 25°C. The blue and grey shades indicate the phase of these genes at 18°C and 25°C respectively. **D.** Total expression of the indicated clock genes in the microarray for each temperature. Only *per* shows a significant difference between 18°C and 29°C.

Figure 2. Temperature modulates *tim* alternative splicing. A. IGV snapshot of the *timeless* locus region indicating the expression of this gene at 18°C (blue), 25°C (black) and 29°C (red). The presented data includes the aggregated data from the 3'-seq datasets presented in Figure 1 (upper traces) as well as full transcript polyA$^+$ RNA seq datasets (lower traces). The latter includes 2 timepoints at 25°C and three timepoints at 18°C and 29°C (see text for details). The arrows indicate the alternative splicing events that are regulated by temperature. **B.** A scheme of the alternatively spliced *tim* isoforms. In grey are constitutive exons, in red sequences found mainly at high temperatures and in blue, sequences found mainly at low temperatures. A zoom on the exons surrounding each non-canonical isoform is represented in the rectangle. Alternative stop codons (STOP) and cleaveage and polyadenylation sites (PAS) in these isoforms are also indicated. **C.** Quantification of the relative amount of *tim-sc* (dark blue), *tim-cold* (light blue), *tim-M* (red) and *tim-L* (grey) isoforms at the three assayed temperatures. To quantify the different isoforms we counted the relative number of spliced junctions specific for each isoform. **D.** Quantification of the relative amount of *per-spliced* (blue) and *per-unspliced* (red) RNAs at the three assayed temperatures performed as in C.

Figure 3. Temperature-specific alternative splicing is conserved across different *Drosophila* species. A. Quantification of the ratio between day and night activity counts of locomotor activity for *D. melanogaster, D. simulans, D. yakuba* and *D. virilis* at 18°C (blue), 25°C (grey) or 29°C (red). Each bar represents the ratio between the mean locomotor activities (light and dark) of all four days (N~32). Significance was calculated performing multiple t-test analysis using the Holm-Sidak method.(*, pval<0.05; **, pval<0.01 ***, pval<0.001; ****, pval<0.0001). **B.** Quantification of the relative amount of *tim-sc* (dark blue), *tim-cold* (light blue), *tim-M* (red) and *tim-L* (grey) from whole transcriptome (polyA$^+$) mRNA-seq in the species at the indicated temperatures. The ratios between the isoforms were calculated as indicated in Figure 2 and explained in the methods section.

Figure 4. Alternatively spliced isoforms of *timeless* are post-transcriptionally regulated. A. *Tim* mRNA is bound to AGO-1 in a temperature dependent way. The graph represents the ranking of enrichment of RNAs in AGO-1 immunoprecipitates isolated from flies entrained at 18°C (blue), 25°C (grey) or 29°C (red). Briefly, we ranked RNAs according to their binding enrichment (lower ranking value corresponds to higher binding to AGO-1). To assess the ranking, we averaged the residuals in a linear model: signal in AGO1-immunoprecipitate/signal in input (n=2 for each temperature). **B.** *tim* isoform-specific qPCR of AGO1-bound mRNAs at 18°C (blue), 25°C (grey) or 29°C (red). Each bar represents an average of all time points normalized to a negative control (*cyc*). Blue starts represent statistical significance to 18°C of the indicated isoform and temperature determined performing multiple t-test analysis using the Holm-Sidak method. (*, pval<0.05; ***, pval<0.001; ****, pval<0.0001). Four different timepoints in each temperature were used as biological replicas. **C.** Luciferase assay of the wings of flies expressing *luciferase* fused to different *tim 3'UTRs*. We utilized the GAL4-UAS system to express the luciferase reporter. In all cases we utilized the *tim-gal* driver. All the UAS-Luciferase lines were inserted in the same genomic location using the Attb system. Blue and grey starts represent statistical significance to *tim-sc* or *tim-L*, respectively, determined by performing multiple t-test analysis using the

Holm-Sidak method. (*, pval<0.05; ***, pval<0.001; ****, pval<0.0001. n=3). **D.** Summary table of the number of miRNAs binding identified in the different *tim* isoforms using TargetScan (Left column). **E.** Volcano plot showing differentially expressed miRNAs between 18°C and 29°C (n = 4 for each temperature). The color code represents the significance for each miRNA differentiating all the combinations for fold change > 2 (FC>2) and padj < 0.05. miRNAs with predicted binding sites present in any of the *tim* isoforms 3'UTR were identified using TargetScanFly.6.2 and are labelled in the graph (blue, grey or red for being putative targets for *tim-cold*, common sequence or *tim-M* 3'UTRs, respectively). miRNA abundance was assessed by small-RNAseq from AGO1 immunoprecipitates. **F.** Relative abundance of miRNAs that are differentially expressed (FC>2 and padj < 0.05) at different temperatures and that are predicted to target the 3' UTR of the different isoforms. For each miRNA, the values have been normalized to the minimum and their relative expression (RE) is represented. miRNA abundance was assessed from small-RNAseq from AGO1 immunoprecipitations.

Figure 5. Over-expression of *tim* isoforms at 25°C results in various behavioral defects. **A.** Actograms of flies of the indicated genotypes in LD12:12 at 25°C. In all cases we over-expressed the indicated isoform utilizing the *tim-gal4* driver. Light phase is represented in white and dark-phase in grey. **B.** Quantification of the start of the evening peak in the last 3 days of LD. Stars represent statistical significance to *tim*-Gal4 control calculated by one-way ANOVA. (*, pval<0.05; **, pval<0.01 ***, pval<0.001; ****, pval<0.0001. n=27-31). **C.** Summary table of the behavior in DD indicating % of rhythmicity, period length, power and their SEM.

Figure 6. *Tim-sc* null flies present behavioral and molecular defects. A. Schematic representation of the mutation performed by CRISPR used to generate *tim-sc* null flies (40A flies). The black and green arrow represent the location of the forward and reverse primers used for the verification of *tim-sc* depletion. **B.** Levels of *tim-sc* after the genetic manipulation depicted in A. The displayed qPCR result was obtained using RNA obtained from heads of flies entrained at 18°C. (n=5). **C.** Average actograms of control (left) and 40A (right) flies at

18°C (blue), 25°C (grey) and 29°C (red) in LD12:12 cycles. (N=23-32). **D.** Ratio between total day and night-time activity at 18°C (blue), 25°C (grey) and 29°C (red) in 12:12LD. Blue and red stars represent statistical significance between flies kept at 18°C or 29°C and those at 25°C, while black ones represent differences to the control flies. Multiple t-test analysis using the Holm-Sidak method. (**, pval<0.01 ***, pval<0.001. n=16-31). **E.** Quantification of the start of the evening peak in day 3 of LD. Blue and red stars represent statistical significance between flies kept at 18°C or 29°C and those at 25°C, while black ones represent differences to the control flies. Multiple t-test analysis using the Holm-Sidak method. (**, pval<0.01 ***, pval<0.001. n=16-31). **F.** Assessment by qPCR of exons5-6 (common in all *tim* isoforms, left) *tim-cold* (middle left), *tim-L* + *tim-M* (middle right) and *tim-M* transcription (right) at 18°C (blue), 25°C (grey) and 29°C (red) at ZT15 in 12:12LD. Multiple t-test analysis using the Holm-Sidak method. (**, pval<0.01 ***, pval<0.001. n=5).

Figure 7. Splicing of *timeless* is temperature dependent and clock independent. A. qPCR results from entrained WT as well as tim^{01} and per^{01} clock mutant flies at 18°C or at 29°C. Each bar represents the ratio between the unspliced and splice variant of *tim-sc* (dark blue), *tim-cold* (light blue), *tim-m* (red) and *tim* control (grey). **B**. *Drosophila* S2 cells transfected with pMT-*Clk* display the same *tim* alternative splicing patterns observed in living flies at 18°C (blue) or at 25°C (grey). Each bar represents the ratio between the unspliced and splice variant of *tim-sc*, *tim-cold*, *tim-m* and *tim* control. Multiple t-test analysis using the Holm-Sidak method. (**, pval<0.01 ***, pval<0.001. n=3). **C.** Scheme of the different *tim* isoform minigenes utilized in (D) and location of the primers used to measure the spliced (top) and unspliced (bottom) of each intron. **D.** Unspliced/spliced ratios for the indicated minigenes at 18°C (blue) or at 25°C (grey). Multiple t-test analysis using the Holm-Sidak method. (**, pval<0.01 ***, pval<0.001. n=3).

Figure 8. Model of the effects of thermosensitive alternative splicing of *timeless* in sensing and mediating temperature adaptation. A. Temperature affects differently each

1209 one of the four *tim* isoforms (*tim-sc, tim-cold, tim-M* and *tim-L*, represented in dark and light
1210 blue, red and grey respectively). While *tim-sc* and *tim-cold* are higher in colder temperatures,
1211 *tim-M* is only expressed at the highest temperatures. Nevertheless, transcription levels of the
1212 canonical isoform, *tim-L*, do not change. **B.** Temperature regulates expression of miRNAs,
1213 which set a threshold to the amount of mRNA that gets translated from each isoform. *tim-sc*
1214 has the lowest and *tim-M* the highest thresholds in all temperatures. *tim-cold*'s has the biggest
1215 temperature-dependent variation. **C.** These differences between the transcript levels and their
1216 thresholds results in changes in TIM expression as well as **D.** behavioral changes in the phase
1217 and day/night ratios that are linked to temperature adaptation.
1218
1219
1220
1221
1222
1223
1224
1225
1226
1227
1228
1229
1230
1231
1232
1233
1234
1235
1236

Supplementary Figure Legends:

Figure S1. Density plot showing the phases of core clock genes cycling at both 29°C and 25°C. The red and grey shades indicate the phase of these genes at 29°C and 25°C respectively.

Figure S2. *Tim* transcription is advanced at 18°C compared to 25°C and 29°C. A. q-RT PCR results for *tim* mRNA, top, or chromatin-bound (nascent RNA) *tim,* bottom, levels on entrained WT fly heads at ZT3, ZT7, ZT11, ZT15, ZT19 and ZT23 (consecutive bars) at 18°C (blue), 25°C (grey) or 29°C (red). **B.** Same as in (A) but for *per*.

Figure S3. Temperature regulates gene expression. A. Heat map showing an unsupervised clustering of differentially expressed genes from a Microarray experiment performed on RNA extracted form entrained fly heads at three temperatures. Each lane represents a mix of all time points at a given temperature. **B.** A pie chart demonstrating enriched GO terms of the differentially expressed genes.

Figure S4. Relative expression of *timRA* and *timRC* in the two DGE described in Figure1. ***ti****m-RA* reports expression levels for *tim-L, tim-cold* and *tim-M,* as they share the 3' end. For Each DGE dataset, we averaged the expression of the different *tim* isoforms over the day at each temperature. Results are shown normalized to 25°C.

Figure S5. *Tim* expression is regulated by temperature co and post-transcriptionalyy. **A.** Isoform-specific q-PCR of *timeless* in the heads of flies entrained at 18°C (blue) and 29°C (red). Each bar represents a different time point (ZT3, ZT9, ZT15 and ZT21). Values have been normalized to the maximum of both temperatures. **B.** Quantification of the different *tim* isoforms in the adult brain at ZT11 after entraining the flies at 18°C (blue), 25°C (grey) and 29°C (red). Black stars represent statistical significance between flies kept at 18°C and those

at 25°C. Multiple t-test analysis using the Holm-Sidak method. **, pval<0.01 ***, pval<0.001. n=16-31. n=3.

Figure S6. Temperature-specific alternative splicing is conserved across different *Drosophila* species. A. IGV snapshot of whole-transcript RNA-seq showing the *tim* locus in three additional species (*D. simulans, D. Yakuba* and *D. virilis*, top to bottom) at different temperatures. The upper panel (blue) corresponds to 18°C, the middle one (black) to 25°C and the lower one to 29°C. Arrows indicate the different areas unique to the different isoforms: *tim-sc* (light blue), *tim-M* (red) and *tim-cold* (blue). Green arrow below the IGV snapshots represent the direction of *tim* transcription. **B.** Quantification of the relative amount of *per*-spliced (light blue), *per*-unspliced (red) and *tim-L* (grey) from whole transcriptome (polyA$^+$) mRNA-seq in all species at the indicated temperatures. The ratios between the isoforms were calculated as indicated in Figure 2 and explained in the methods section.

Figure S7. Density plot representing 4000 genes, selected as 'AGO1-enriched/associated'. The distributions represent the frequency of each fold enrichment for a particular temperature.

Figure S8. Overexpression of different *tim* isoforms with FLAG-tagged C-terminus. A. Schematic representation of TIM protein. The starts mark the location of the different FLAG-tags for each isoform. NLS: Nuclear Localization Signal. CLD: Cytoplasmic Localization Domain. **B.** Western blot membranes showing anti-FLAG and anti-TIM staining of the over-expression of the four 3' FLAG-tagged UAS-*tim* isoforms in S2 cells. Arrows mark a degradation product ~ 60kDa smaller than the original TIM isoform.

Figure S9. Total activity counts in control and 40A mutant flies at 18°C (blue), 25°C (grey) and 29°C(red) in LD12:12 during the day (left) and night (right). Stars represent

1291 significant differences between the control and mutants from the same temperature. Multiple
1292 t-test analysis using the Holm-Sidak method. **, pval<0.01 ***, pval<0.001. N=23-32.
1293
1294 **Figure S10. Summary table of the 3' and 5' splicing strengths of each *tim* intron for**
1295 ***Drosophila melanogaster, Drosophila simulans* and *Drosophila virilis.***
1296
1297
1298
1299
1300
1301
1302
1303
1304
1305
1306
1307
1308
1309
1310
1311
1312
1313
1314
1315
1316

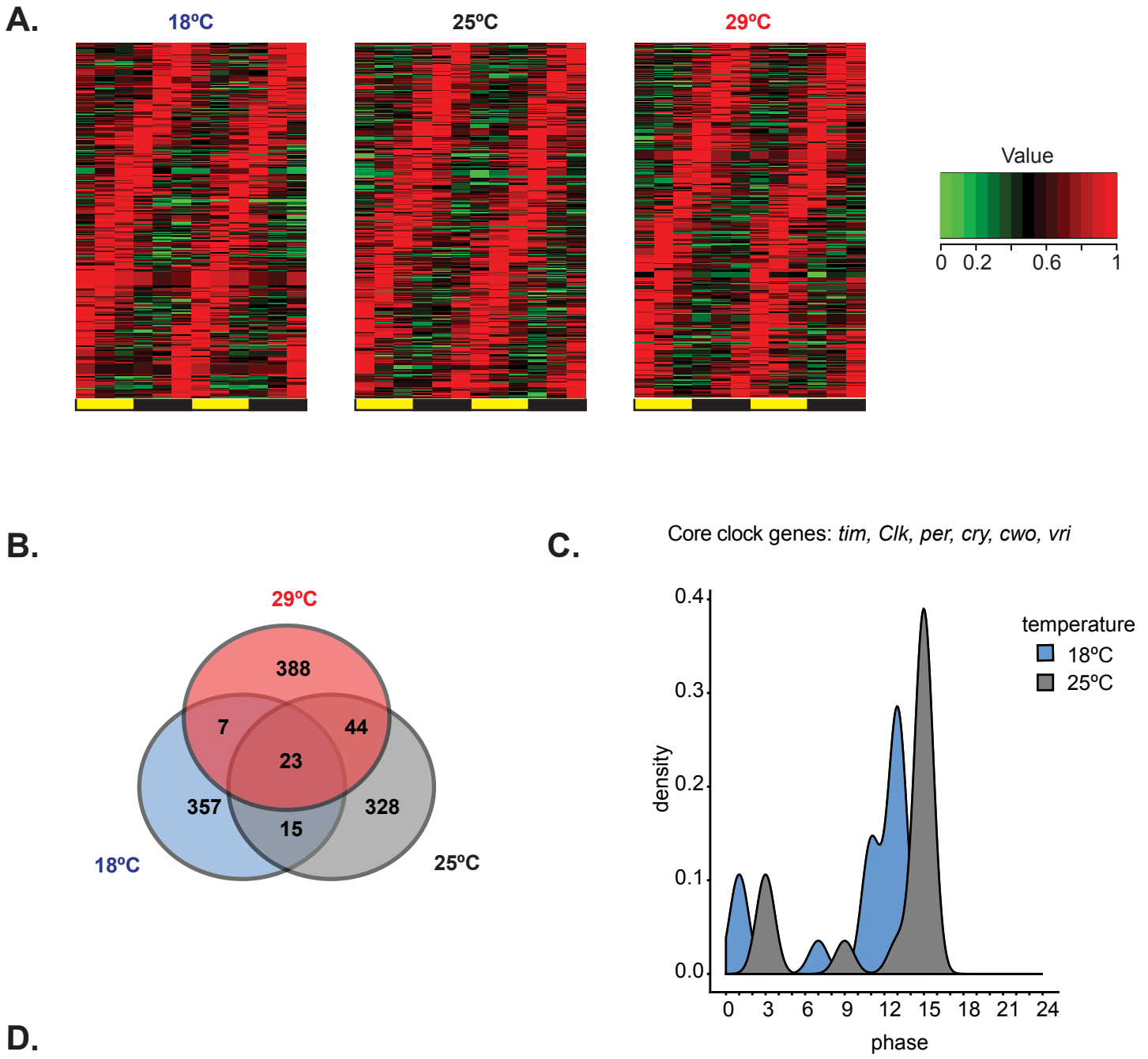
A.
18ºC
25ºC
29ºC
Value
0
0.2
0.6
1
B.
29ºC
388
7
44
23
357
328
15
18ºC
25ºC
C.
Core clock genes: tim, Clk, per, cry, cwo, vri
temperature
18ºC
25ºC
density
0.4
0.3
0.2
0.1
0.0
0
3
6
9
12
15
18
21
24
phase
D.
18ºC
25ºC
29ºC
Total expression
300
200
100
0
timRA
per
cyc
vri
cry
cwo
Clk

Figure 1

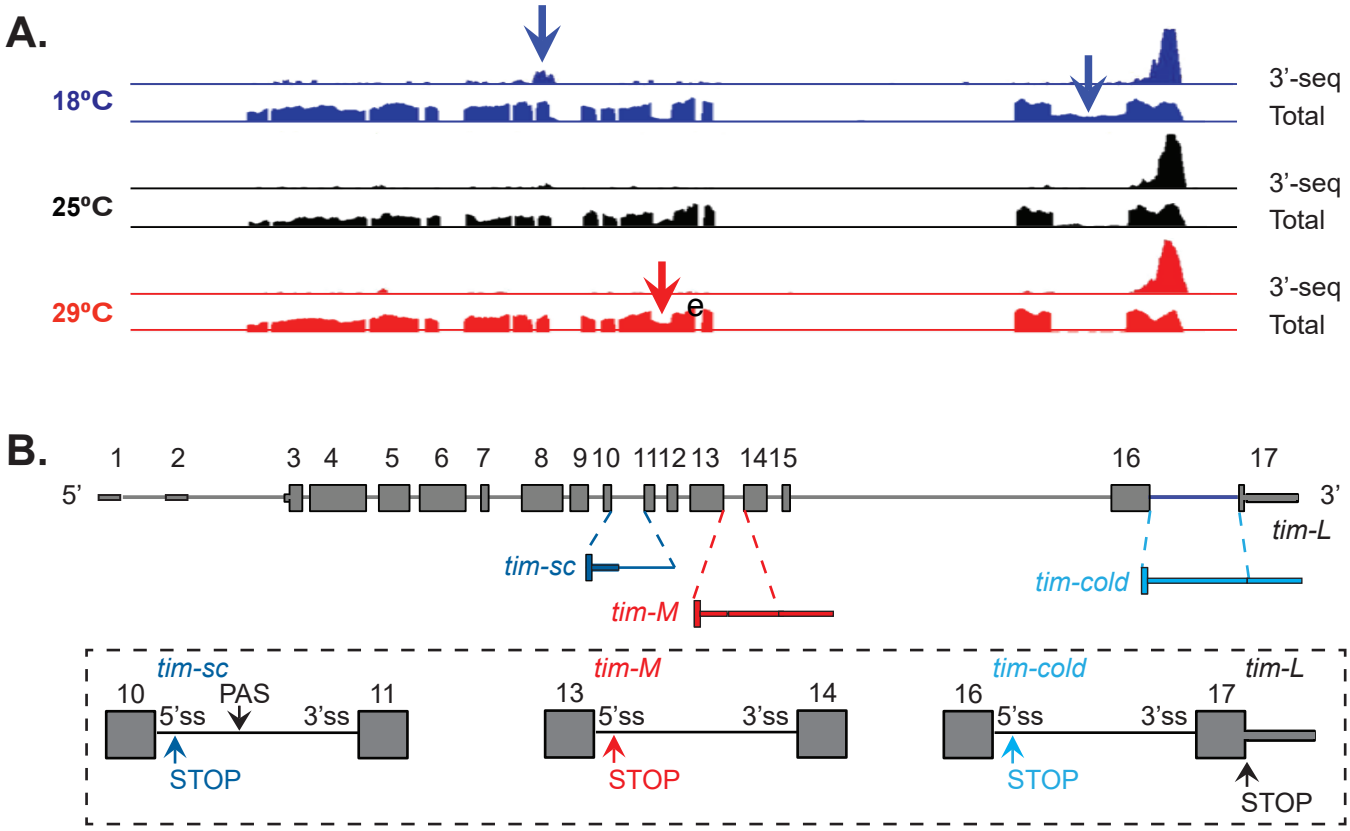
A.
18ºC
25ºC
29ºC
3'-seq
Total
3'-seq
Total
3'-seq
Total
e
B.
1 2 3 4 5 6 7 8 9 10 11 12 13 14 15 16 17
5'
3'
tim-L
tim-sc
tim-cold
tim-M
tim-sc
PAS
10
5'ss
3'ss
11
STOP
tim-M
13
5'ss
3'ss
14
STOP
tim-cold
tim-L
16
5'ss
3'ss
17
STOP
STOP
C.
tim splicing isoforms
% of isoforms
100
80
60
40
20
0
18ºC
25ºC
29ºC
tim-sc
tim-cold
tim-L
tim-M
D.
per splicing isoforms
% of isoforms
100
80
60
40
20
0
18ºC
25ºC
29ºC
spliced
unspliced

Figure 2

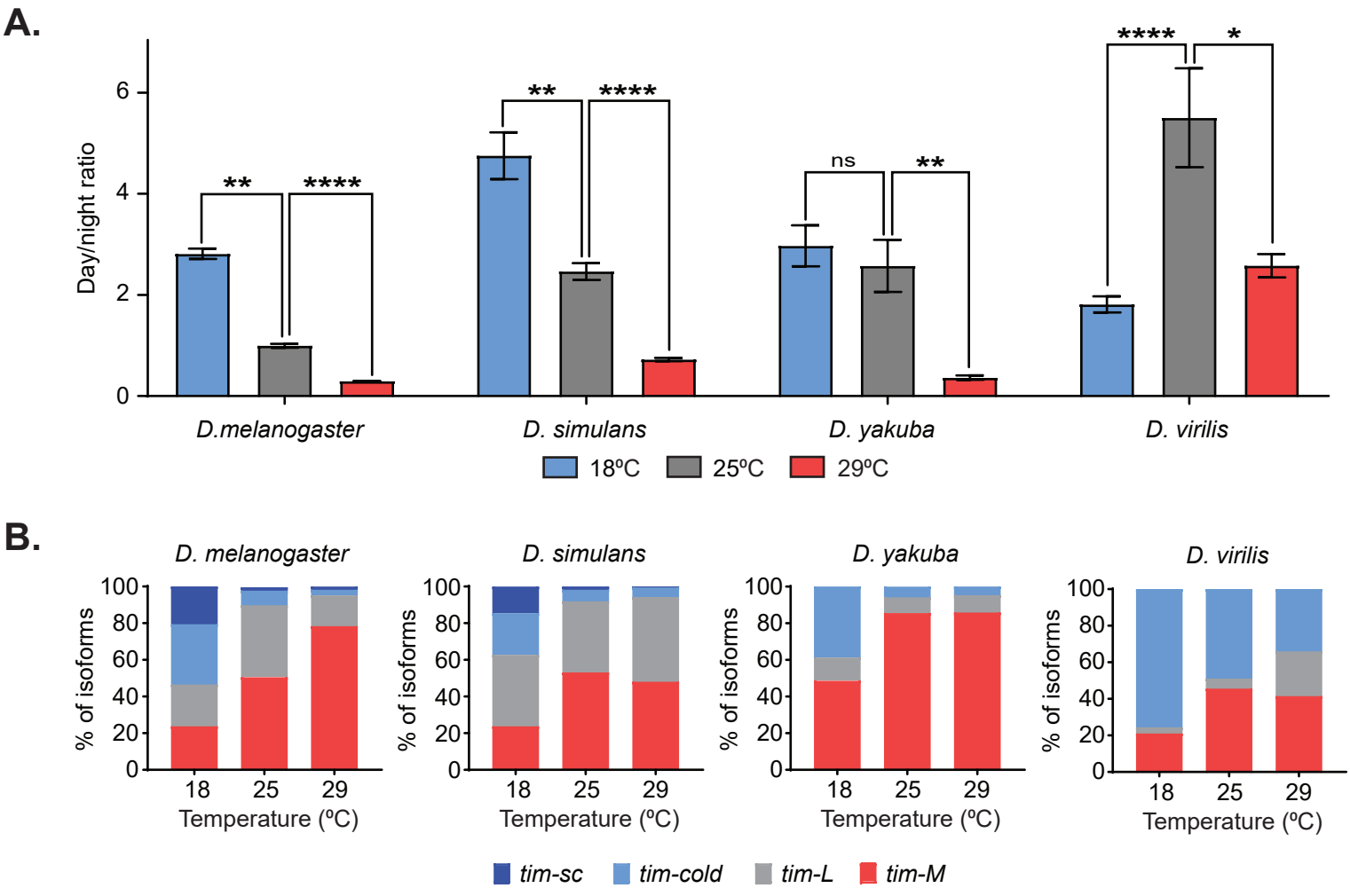
A.
Day/night ratio
0
2
4
6
**
****
**
****
ns
**
****
*
D.melanogaster
D. simulans
D. yakuba
D. virilis
18ºC
25ºC
29ºC
B.
D. melanogaster
D. simulans
D. yakuba
D. virilis
% of isoforms
0
20
40
60
80
100
18
25
29
Temperature (ºC)
tim-sc
tim-cold
tim-L
tim-M

Figure 3

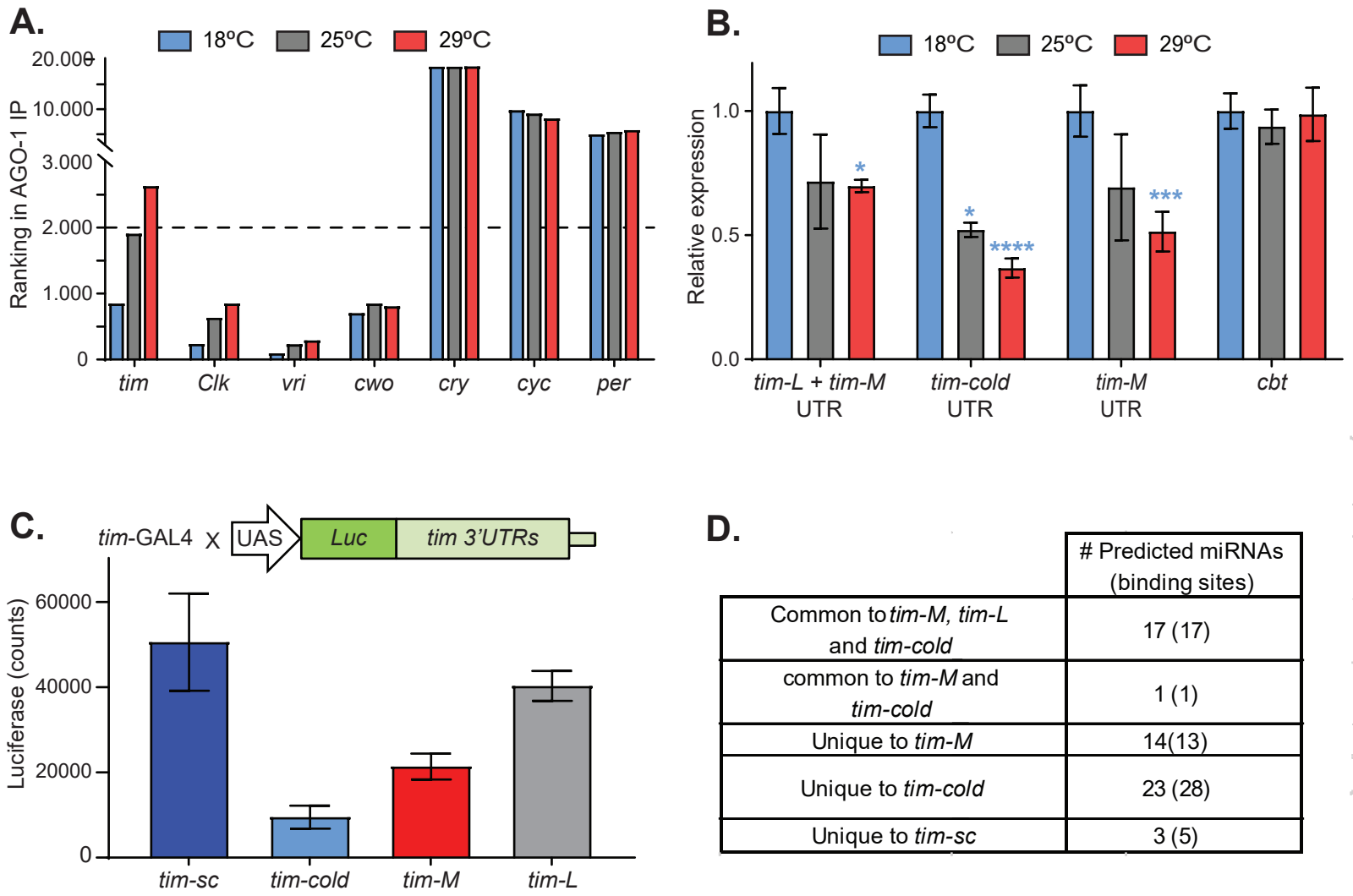
A.
18ºC
25ºC
29ºC
Ranking in AGO-1 IP
20.000
10.000
3.000
2.000
1.000
0
tim
Clk
vri
cwo
cry
cyc
per
B.
18ºC
25ºC
29ºC
Relative expression
1.0
0.5
0.0
*
*
****
***
tim-L + tim-M UTR
tim-cold UTR
tim-M UTR
cbt
C.
tim-GAL4 X
UAS
Luc
tim 3'UTRs
Luciferase (counts)
60000
40000
20000
0
tim-sc
tim-cold
tim-M
tim-L
D.
Predicted miRNAs (binding sites)
Common to tim-M, tim-L and tim-cold
17 (17)
common to tim-M and tim-cold
1 (1)
Unique to tim-M
14(13)
Unique to tim-cold
23 (28)
Unique to tim-sc
3 (5)
E.
dme-miR-33-5p
dme-miR-4919-3p
dme-miR-284-5p
dme-miR-92b-3p
dme-miR-210-5p
dme-miR-375-5p
dme-miR-2a-2-5p
dme-miR-4976-5p
dme-miR-1001-3p
dme-miR-969-3p
lfc
FC>2
no
pv<.05
p<.05 FC>2
-log10(padj)
30
20
10
0
-2.5
0.0
2.5
5.0
7.5
log2FoldChange
F.
Common to tim-L + tim-M + tim-cold
RE
4
2
0
miR-969
miR-33
18ºC
25ºC
29ºC
Unique to tim-cold
RE
4
2
0
miR-1001
miR-210
miR-284
miR-92b
Unique to tim-M
RE
8
6
4
2
0
miR-210
miR-2a-2
miR-375
miR-33
miR-4919
miR-4976

Figure 4

A.

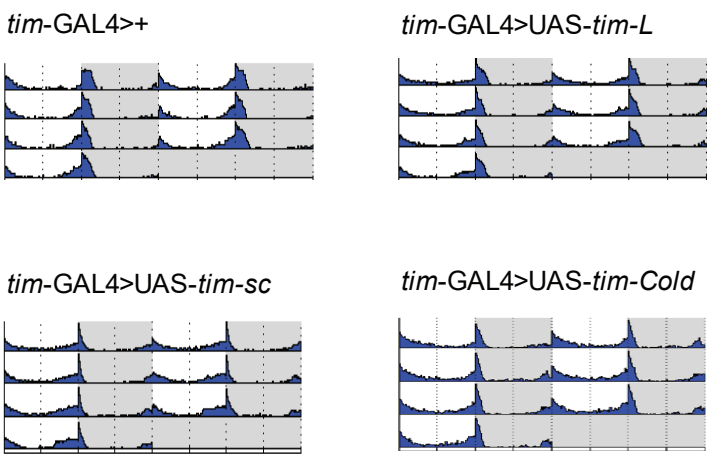

B.

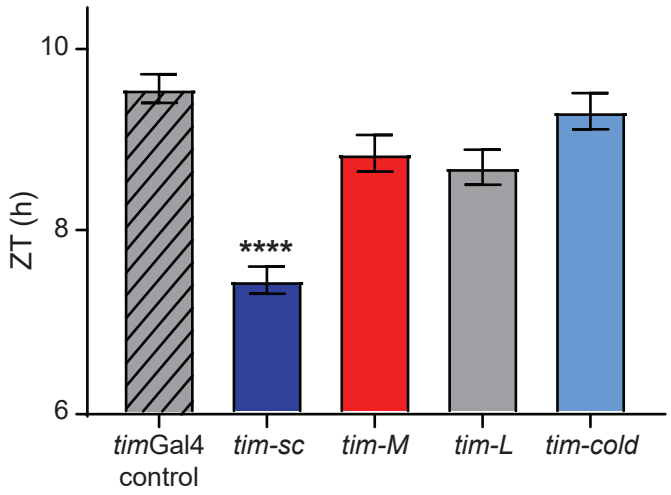

C.

Genotype	Rhythmicity	Period Mean (h)	Period SEM	Power Mean	Power SEM	n
tim-GAL4>+	96.9	24.7	0.1	326.5	13.5	32
tim-GAL4>UAS-*tim-L*	90.3	26.1	0.9	203.9	21.1	31
tim-GAL4>UAS-*tim-M*	100.0	24.5	0.1	471.8	25.9	32
tim-GAL4>UAS-*tim-Cold*	100.0	25.0	0.4	223.0	15.1	27
tim-GAL4>UAS-*tim-sc*	100.0	23.3	0.1	475.4	41.3	30

Figure 5

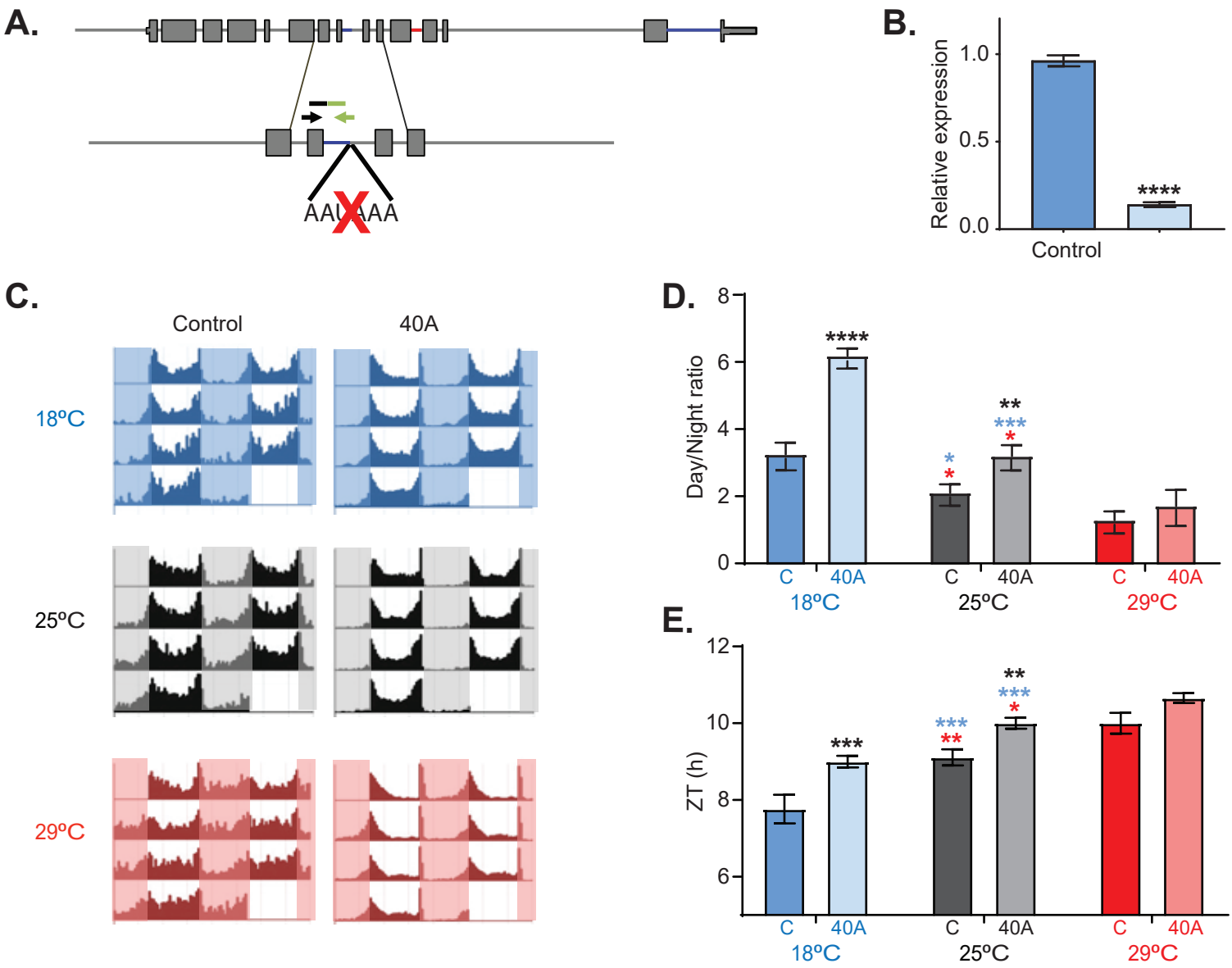
A.
AAUAAA
B.
Relative expression
1.0
0.5
0.0
****
Control
C.
Control
40A
18ºC
25ºC
29ºC
D.
Day/Night ratio
8
6
4
2
0
****
**
***
*
C
40A
18ºC
25ºC
29ºC
E.
ZT (h)
12
10
8
6
***
**
*
F.
tim common
tim-cold
tim-M + tim-L
tim-M
2.0
1.5
1.0
0.5
0.0
C 40A
18ºC
25ºC
29ºC

Figure 6

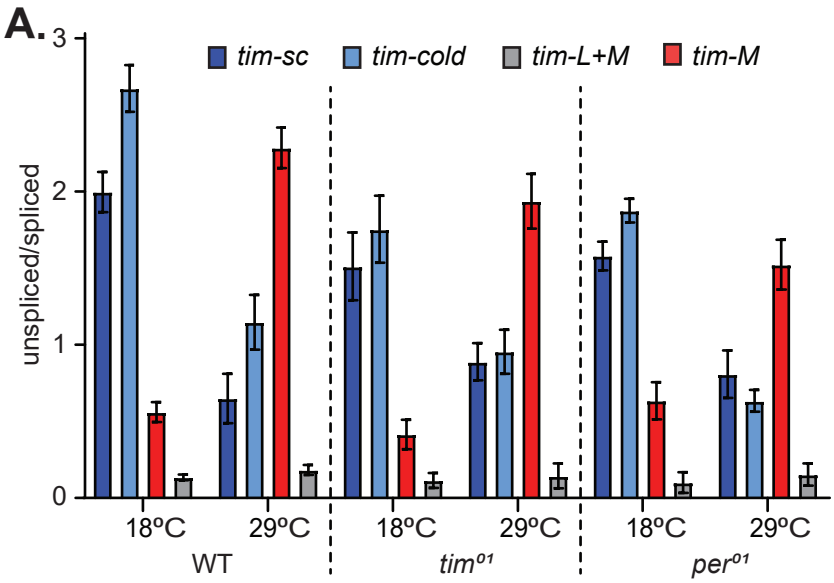
A.
tim-sc
tim-cold
tim-L+M
tim-M
unspliced/spliced
3
2
1
0
18ºC
29ºC
18ºC
29ºC
18ºC
29ºC
WT
tim01
per01

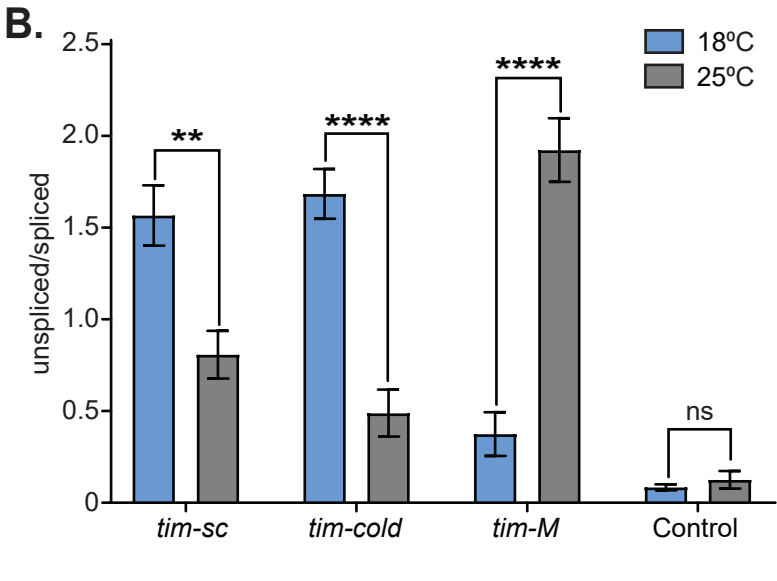
B.
18ºC
25ºC
unspliced/spliced
2.5
2.0
1.5
1.0
0.5
0
**
****
****
ns
tim-sc
tim-cold
tim-M
Control

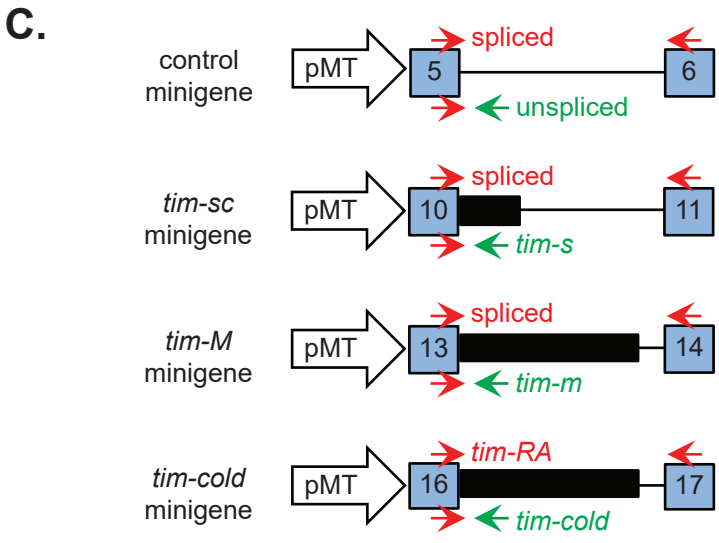
C.
control minigene
pMT
5
6
spliced
unspliced
tim-sc minigene
10
11
tim-s
tim-M minigene
13
14
tim-m
tim-cold minigene
16
17
tim-RA
tim-cold

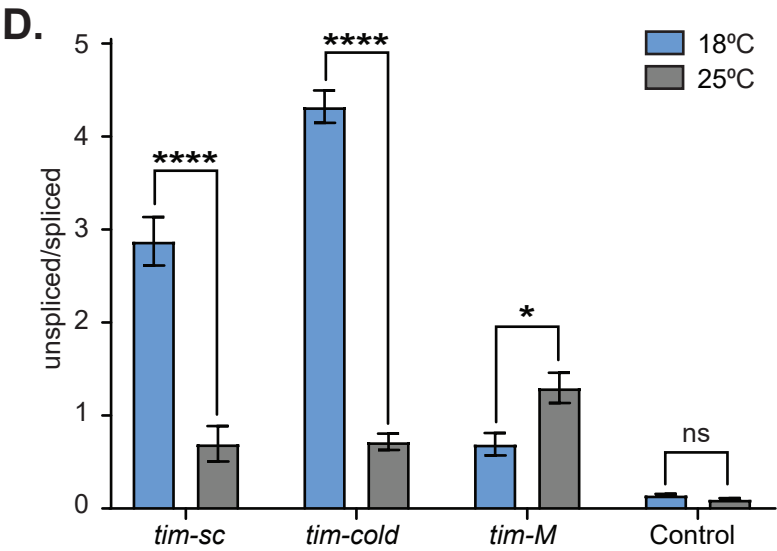
D.
18ºC
25ºC
unspliced/spliced
5
4
3
2
1
0
****
****
*
ns
tim-sc
tim-cold
tim-M
Control

Figure 7

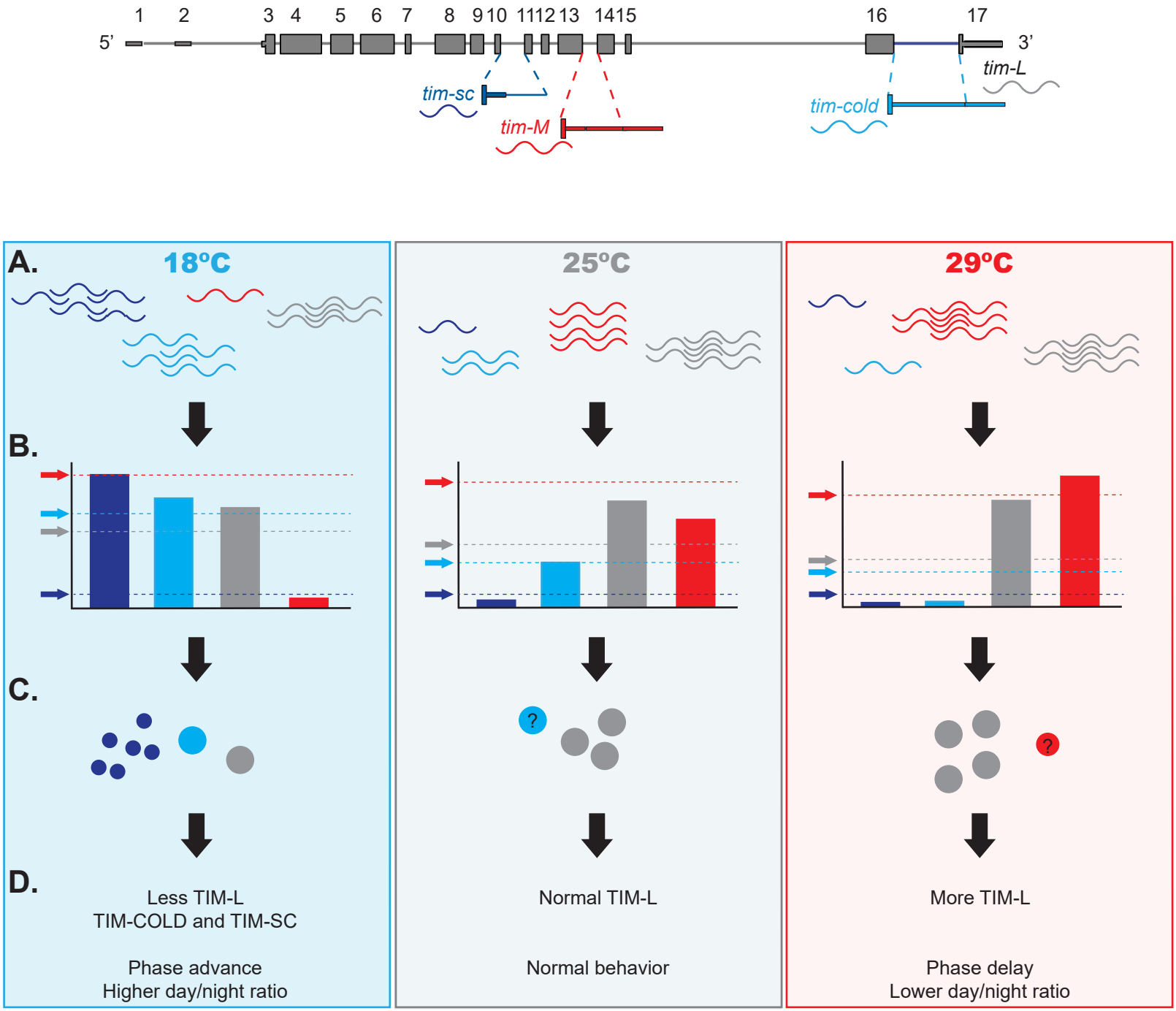
1 2 3 4 5 6 7 8 9 10 11 12 13 14 15 16 17
5'
3'
tim-sc
tim-M
tim-cold
tim-L
A.
18°C
25°C
29°C
B.
C.
?
?
D.
Less TIM-L
TIM-COLD and TIM-SC
Phase advance
Higher day/night ratio
Normal TIM-L
Normal behavior
More TIM-L
Phase delay
Lower day/night ratio

Figure 8

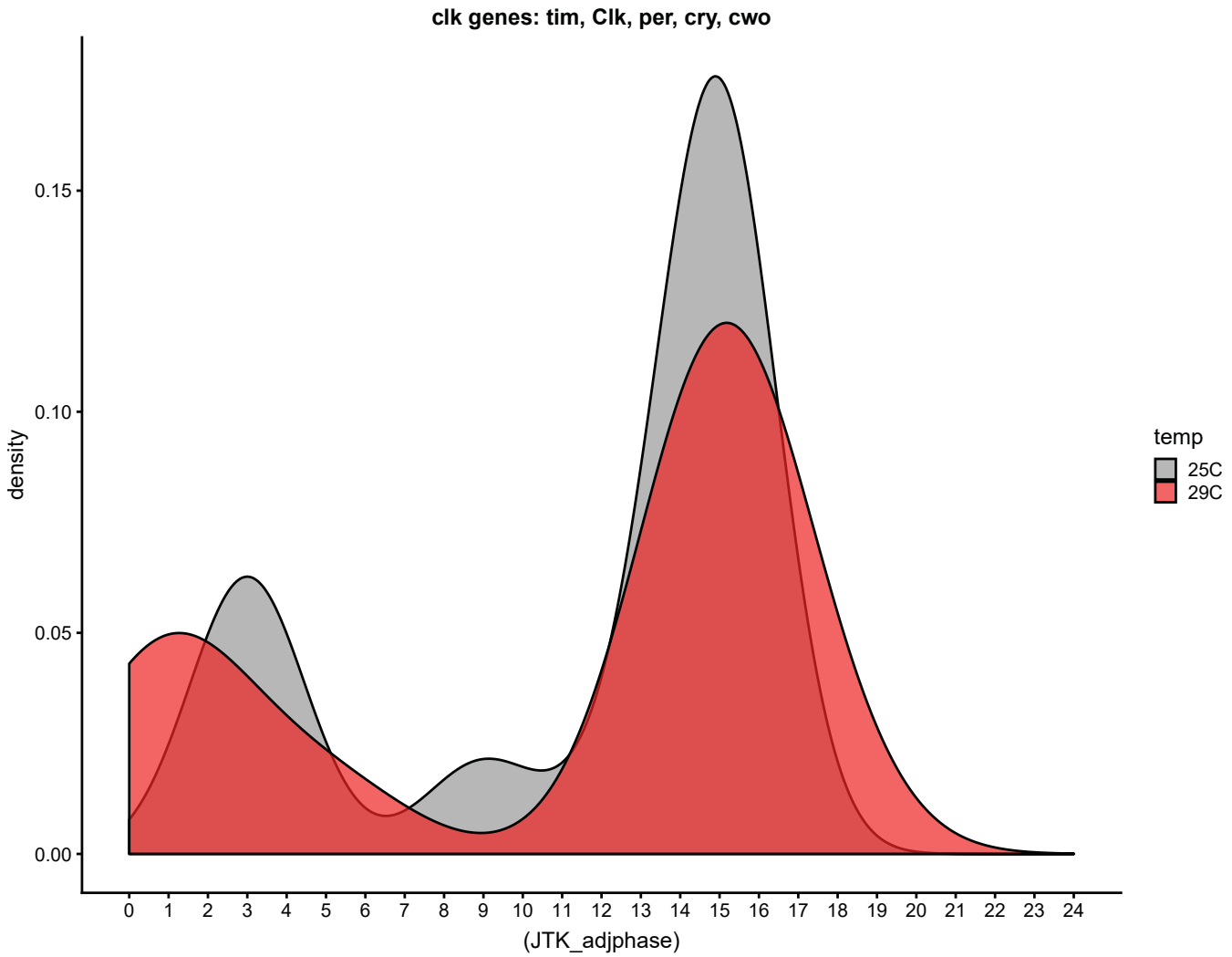

Figure S1

A.

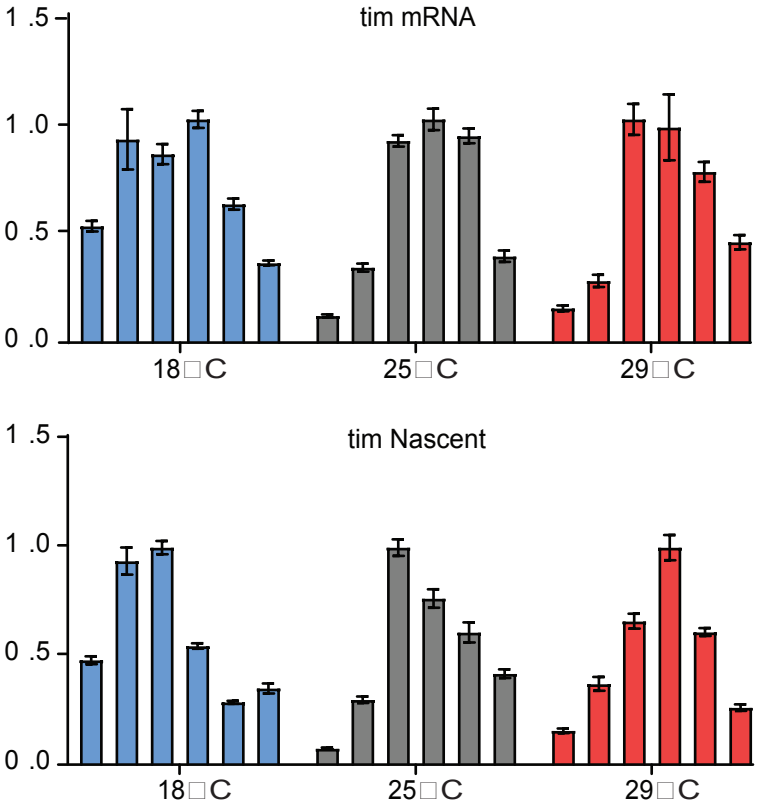
tim mRNA
1 .5
1 .0
0 .5
0 .0
18□C
25□C
29□C
tim Nascent
1 .5
1 .0
0 .5
0 .0
18□C
25□C
29□C

B.

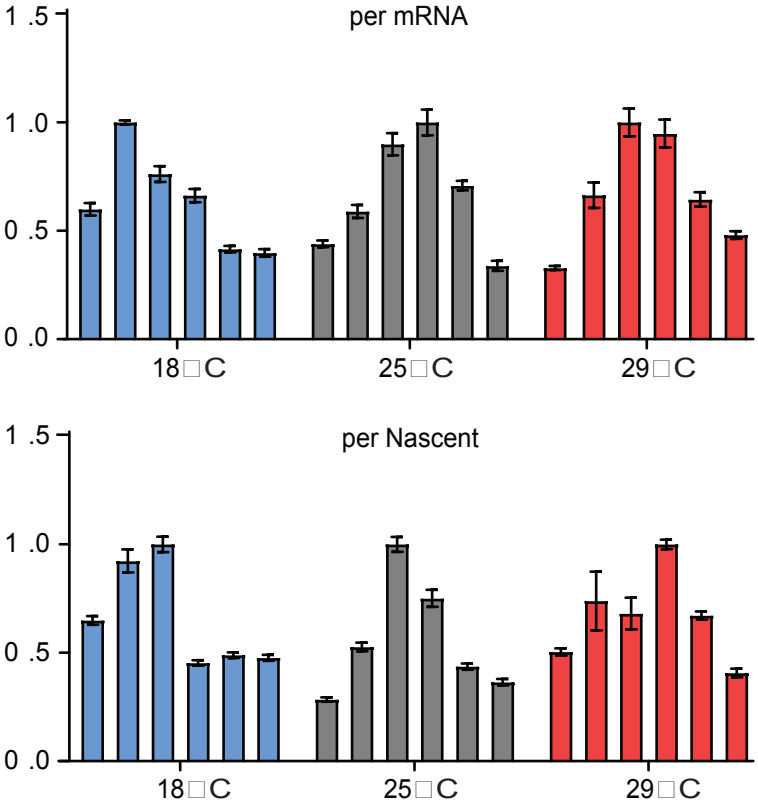
per mRNA
1 .5
1 .0
0 .5
0 .0
18□C
25□C
29□C
per Nascent
1 .5
1 .0
0 .5
0 .0
18□C
25□C
29□C

Figure S2

A.

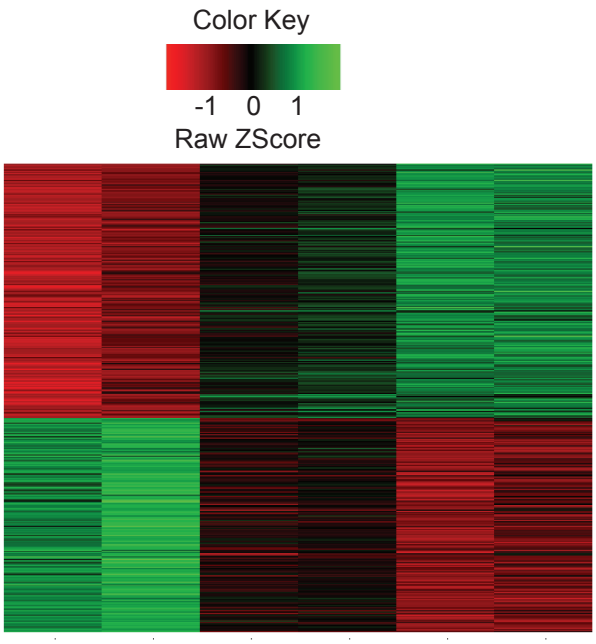
Color Key
-1 0 1
Raw ZScore

B.

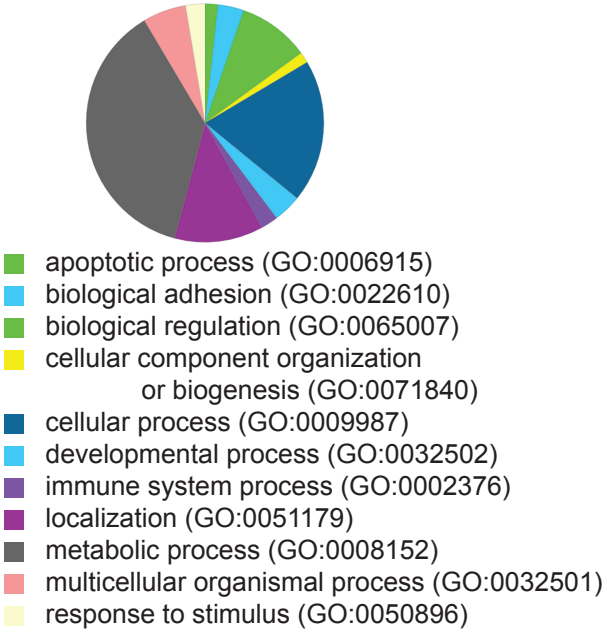
apoptotic process (GO:0006915)
biological adhesion (GO:0022610)
biological regulation (GO:0065007)
cellular component organization
or biogenesis (GO:0071840)
cellular process (GO:0009987)
developmental process (GO:0032502)
immune system process (GO:0002376)
localization (GO:0051179)
metabolic process (GO:0008152)
multicellular organismal process (GO:0032501)
response to stimulus (GO:0050896)

Figure S3

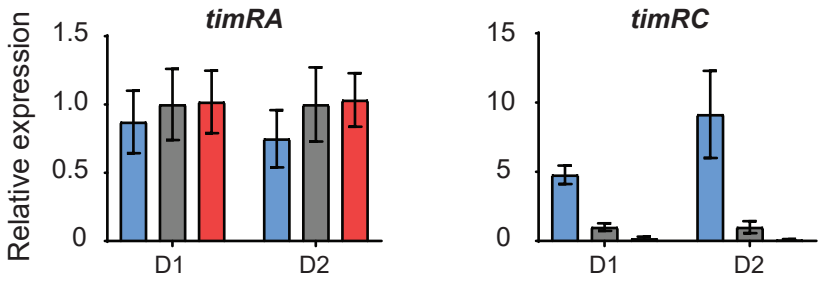

Figure S4

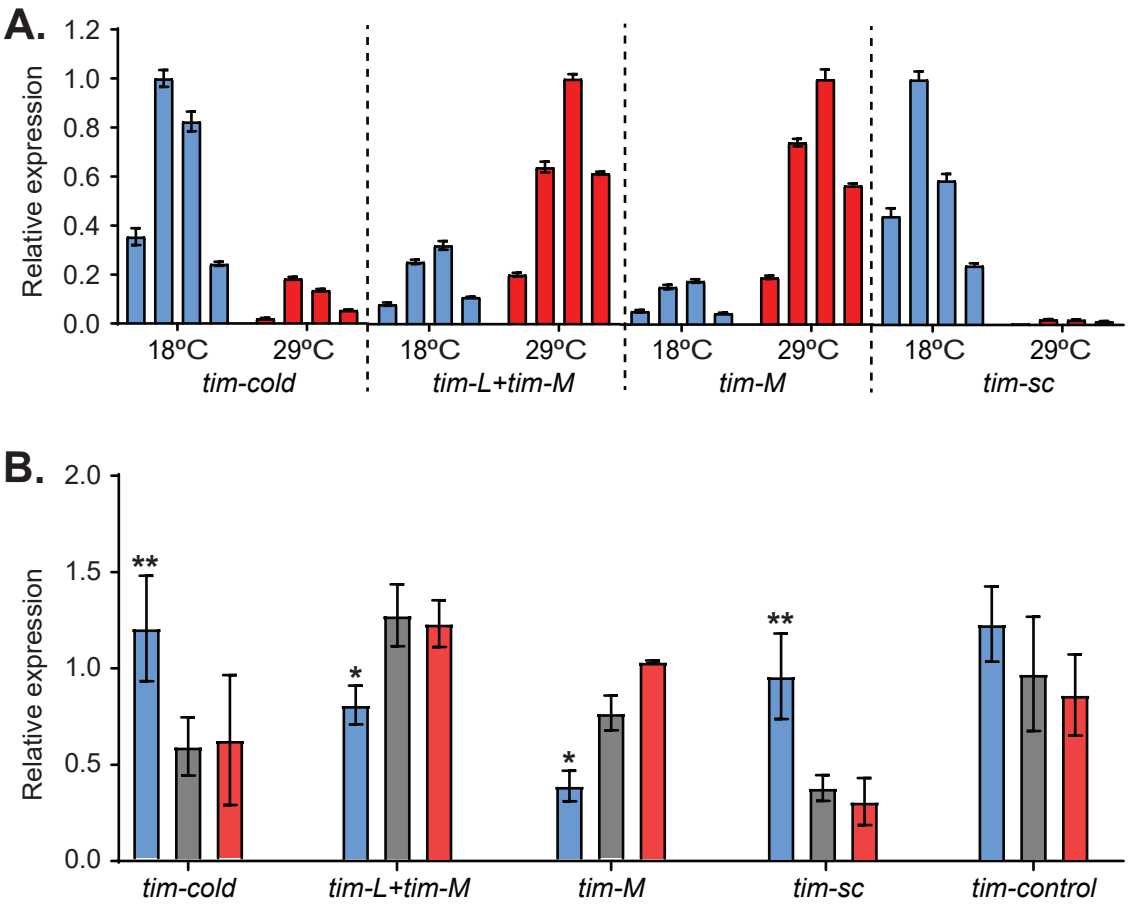
A.
Relative expression
1.2
1.0
0.8
0.6
0.4
0.2
0.0
18ºC
29ºC
18ºC
29ºC
18ºC
29ºC
18ºC
29ºC
tim-cold
tim-L+tim-M
tim-M
tim-sc
B.
Relative expression
2.0
1.5
1.0
0.5
0.0
**
*
*
**
tim-cold
tim-L+tim-M
tim-M
tim-sc
tim-control

Figure S5

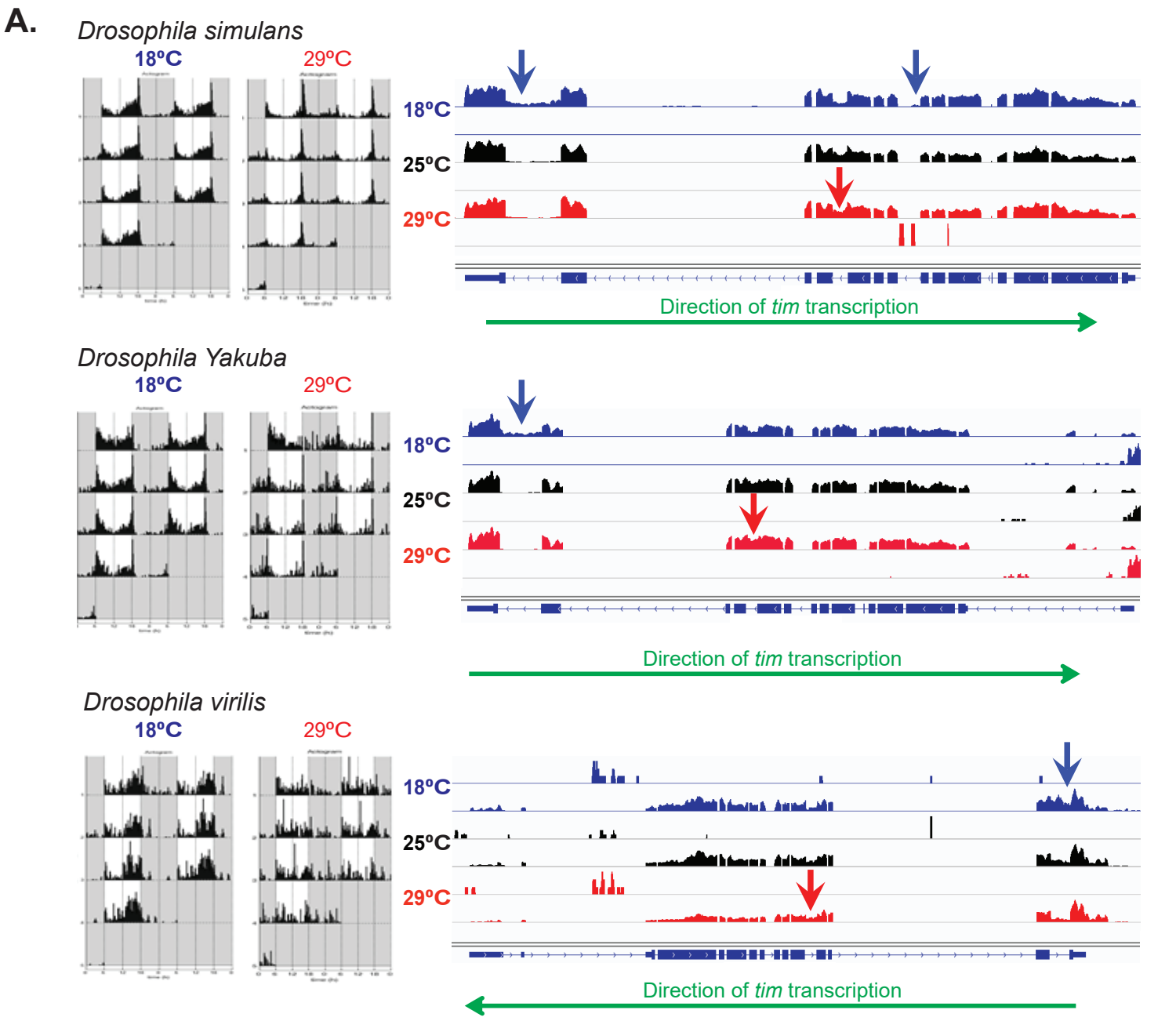
A.
Drosophila simulans
18ºC
29ºC
18ºC
25ºC
29ºC
Direction of tim transcription
Drosophila Yakuba
18ºC
29ºC
18ºC
25ºC
29ºC
Direction of tim transcription
Drosophila virilis
18ºC
29ºC
18ºC
25ºC
29ºC
Direction of tim transcription
B.
D. melanogaster
D. simulans
D. yakuba
D. virilis
% of isoforms
100
80
60
40
20
0
18
25
29
Temperature (ºC)
per unspliced
per spliced

Figure S6

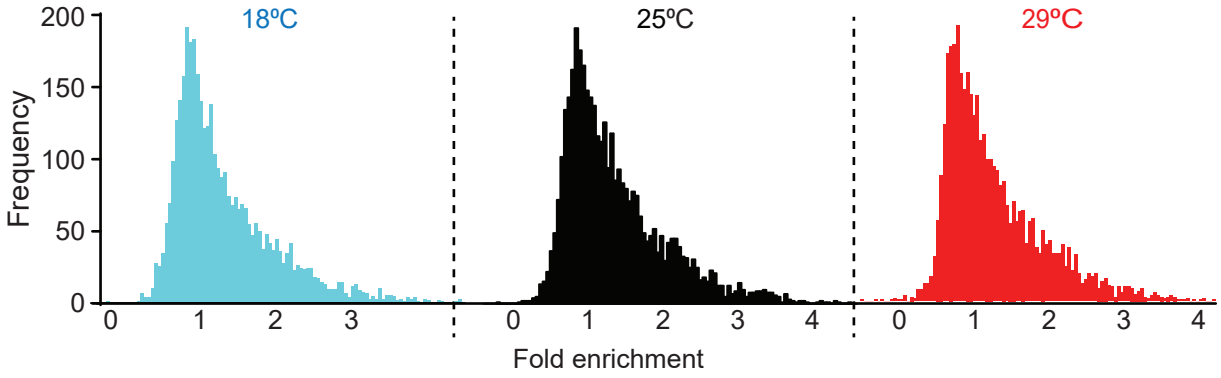
18ºC
25ºC
29ºC
Frequency
200
150
100
50
0
0
1
2
3
0
1
2
3
4
0
1
2
3
4
Fold enrichment

Figure S7

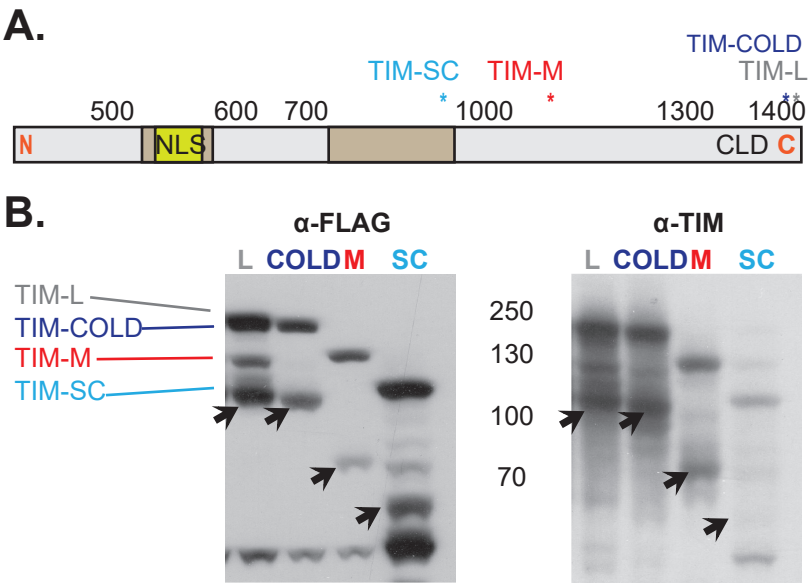
A.
TIM-COLD
TIM-SC
TIM-M
TIM-L
500
600
700
1000
1300
1400
N
NLS
CLD
C
B.
α-FLAG
α-TIM
L
COLD
M
SC
TIM-L
TIM-COLD
TIM-M
TIM-SC
250
130
100
70

Figure S8

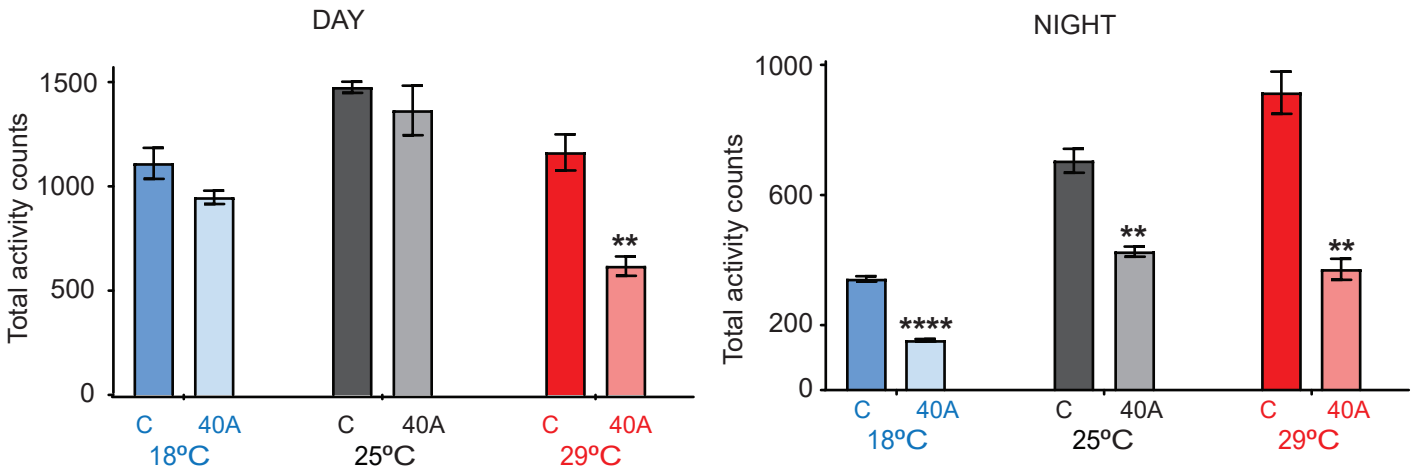
DAY
Total activity counts
1500
1000
500
0
**
C
40A
18ºC
C
40A
25ºC
C
40A
29ºC
NIGHT
Total activity counts
1000
600
200
0
****
**
**
C
40A
18ºC
C
40A
25ºC
C
40A
29ºC

Figure S9

D. melanogaster		
Intron #	5' SS	3' SS
2	0.92	0.97
3	0.93	0.84
4	0.98	0.97
5	0.90	0.82
6	0.82	0.69
7	0.29	0.98
8	0.92	0.94
9	0.88	0.96
10	0.69	0.58
11	0.94	0.97
12	0.90	0.32
13	0.95	0.88
14	0.94	0.93
15	0.76	0.22

D. simulans		
Intron #	5' SS	3' SS
2	0.96	0.92
3	0.98	0.98
4	0.89	0.62
5	0.82	0.59
6	0.03	---
7	0.22	0.93
8	0.92	0.88
9	0.88	0.96
10	0.76	0.92
11	0.96	0.94
12	0.90	0.18
13	0.95	0.75
14	0.94	0.95
15	0.76	0.22

D. yakuba		
Intron #	5' SS	3' SS
2		
3	0.85	0.20
4	0.93	0.98
5	0.88	0.89
6	0.91	0.91
7	0.22	0.97
8	0.88	0.79
9	0.88	0.94
10	0.98	0.60
11	0.90	0.34
12	0.95	0.84
13	0.82	0.84
14	0.79	0.13

	5' SS	3' SS
Short 1st	0.62	0.74
Long 1st	0.54	

Figure S10

Table S1. Circadian oscillation analysis. The circadian analysis was performed using the MetaCycle algorithm (see main text for details). In the table the p-value, phase and amplitude are reported for each gene along with its normalized expression at each circadian timepoint.

Table S2. Gene ontology analysis for the genes with circadian oscillation at each temperature. Genes are ordered by ranking in Fisher exact test. Three different ontologies were analyzed: Biological process. Molecular function. Cellular component. Top 100 genes are reported.

Table S3. Predicted miRNA binding sites (using TargetScan) for each *tim* RNA isoform 3' UTR. Putative miRNA binding sites are reported given the chromosome coordinates. Conservation in different insect species is also reported.

Table S4. Differential miRNA expression at each temperature. Log2(fold change) and p-adjusted value from DeSeq2 are reported for each miRNA.